NASA Technical Paper 1481

Light Airplane Crash Tests at Three Pitch Angles

Victor L. Vaughan, Jr., and Emilio Alfaro-Bou

NOVEMBER 1979

NASA

NASA Technical Paper 1481

Light Airplane Crash Tests at Three Pitch Angles

Victor L. Vaughan, Jr., and Emilio Alfaro-Bou
Langley Research Center
Hampton, Virginia

National Aeronautics
and Space Administration

**Scientific and Technical
Information Branch**

1979

CONTENTS

SUMMARY

Three general-aviation airplane specimens were crash tested at the Langley impact dynamics research facility under controlled free-flight conditions. The nominal test parameters were ground-contact pitch angles of -15° (pitch-down), 0° (flat), and 15° (pitch-up); a flight-path angle of -15°; and a flight-path velocity of 27 m/sec. The pitch angle of the airplane was the only parameter varied, although other factors such as flight-path angle, roll, yaw, velocity, angular rates, impact surfaces, and fire can affect airplane crash behavior.

The crash tests revealed three different dynamic reactions at impact. The pitch-down test specimen made ground contact on the fuselage nose, and a second impact or slam down occurred as the fuselage rotated down and the cabin area contacted the ground; the flat test specimen made a single ground contact in the cabin area; and the pitch-up test specimen made ground contact on the aft end of the fuselage and rocked forward onto the nose. The cabin floor in the vicinity of the third window location sustained considerably more damage and higher accelerations in the flat and pitch-up test specimens than in the pitch-down test specimen. Livable cabin volumes were maintained in all three tests. The longitudinal accelerations on the passenger-compartment floor were greatest in the flat test specimen and lowest in the pitch-down test.

The physical damage to the passenger compartment increases from the pitch-down to the pitch-up test attitudes. This increase in physical damage is accompanied by an increase in structural peak accelerations on the floor of the airplane. These peak accelerations, however, do not generally occur at the same locations on the compartment floor. The peak pelvic accelerations in the first-passenger dummy decreased as the fuselage structural damage increased.

INTRODUCTION

With the rapid growth of private and commercial air traffic since World War II, increasing emphasis has been focused on the causes of passenger injuries and death in severe but potentially survivable crashes. NACA (National Advisory Committee for Aeronautics), the predecessor of NASA (National Aeronautics and Space Administration), conducted a series of full-scale airplane crash tests with instrumented dummies in the early 1950's (refs. 1 and 2). These tests were performed by accelerating the airplane along a horizontal guide rail and crashing it into an earthen mound. Later NACA studies on the dynamic response of seat structures to impact loads (ref. 3) resulted in a CAA (Civil Aeronautics Administration) update in static seat-strength requirements. The airplanes previously tested by NACA, however, were not structurally representative of current general-aviation airplanes.

In 1973, a joint general-aviation crash-test program was initiated by NASA and the FAA (Federal Aviation Administration) (ref. 4). As part of this new program, NASA Langley Research Center is conducting a series of full-scale

crash tests to obtain information on airplane crashes under controlled conditions. Two objectives of the program are to understand what happens inside modern airplanes during a simulated crash and to learn how various crash parameters affect the magnitude and pattern of structural damage. This information is essential for predicting structural collapse and for designing new concepts for seats, occupant restraint systems, and cabin interiors. The variations in planned impact parameters for twin-engine airplanes are shown in table I.

There are certain lethal crashes in which the airplane structure is damaged beyond hope of occupant survivability. Langley's crash studies are not directed toward such crash conditions, but rather toward those crashes in which the airplane structure retains sufficient cabin volume and a potential for occupant survivability.

This report describes the results of three crash tests conducted with nominal ground-contact pitch angles of -15°, 0°, and 15°, a nominal flight-path angle of -15°, and a nominal flight-path velocity of 27 m/sec. The effect of pitch angle at impact is discussed in terms of structural damage and accelerations. The effects of other parameters such as roll, yaw, angular rates, flight-path velocities, various impact surfaces, and fire are not covered in this report. The effects of impact velocity, flight-path angle, and roll are discussed in references 5 to 7, respectively.

The present tests were not conducted to evaluate the crash dynamics of a specific airplane but rather to obtain a data base of crash information on structural damage and to assess analytical predictions of structural components and seat/occupant behavior. A motion-picture film supplement of these tests at the three different pitch angles is available on loan. A request card form and a description of the film are found at the back of this paper.

TEST FACILITY AND PROCEDURES

Facility

The crash tests were performed at the Langley impact dynamics research facility shown in figure 1. The gantry is composed of truss elements arranged with three sets of inclined legs to give vertical and lateral support and another set of inclined legs to provide longitudinal support. The gantry is 73 m high and 122 m long. The supporting legs are spread 81 m apart at the ground and 20 m apart at the 66-m level. An enclosed elevator and a stairway provide access to the overhead work platforms, and catwalks permit safe traverse of the upper levels of the gantry. A movable bridge spans the gantry at the 66-m level and traverses the length of the gantry. Shown in figure 2 is a sketch of a full-scale airplane specimen suspended from the gantry in the ready position to be swung onto the impact surface. The reinforced concrete impact surface was selected to provide repeatability for the test and to allow comparison between tests conducted on the same impact surface. Detailed information on the facility systems necessary to carry out a successful aircraft crash test is reported in reference 8.

Airplane Crash-Test Technique

The test technique used to crash the airplane specimens is shown schematically in figure 3. The airplane, suspended by two swing cables attached to the top of the gantry, is drawn back above the impact surface by a pullback cable to a height of about 49 m. The test sequence is initiated when the airplane is released from the pullback cable. The airplane swings pendulum style onto the impact surface. The swing cables are pyrotechnically separated from the airplane when the airplane is about 1 m above the impact surface in order to free it from restraint during the crash impact. The umbilical cable remains attached during the impact for data acquisition and is pyrotechnically separated about 0.75 sec after swing-cable separation.

Airplane Suspension System

The airplane suspension system used to control the swing of the airplane is shown in figure 4. The swing and pullback cables connect to the swing and pullback harnesses. The swing harness consists of two swing-cable extensions which attach to the wing hard points to support the airplane and to control roll. There are two sets of pitch cables that connect to the swing-cable rings and to fuselage hard points fore and aft of the airplane center of gravity to control the angle of attack. The interaction of all cables in the harness system is involved in yaw control. The pullback harness consists of the two harness cables attached to the wing hard points and to the pullback cable. A bar spreads the cables to clear the fuselage. The pullback cable attached to this harness is used to pull the airplane to the height necessary to produce an impact velocity of 27 m/sec along the flight path. An umbilical cable links the accelerometers to a data-acquisition system located in a building adjacent to the gantry.

Test Parameters

The flight-path angle and attitude angles for the airplane are identified in figure 5, along with the axes and force directions. The actual test parameters for the three tests reported herein, along with photographs of the impact attitude for each airplane test specimen, are presented in figure 6. All impact parameters were nominally the same, except for angle of attack and pitch angle. For consistency and brevity, each test and airplane specimen will hereafter be identified by word descriptions for pitch angle (i.e., pitch-down (-15° test), flat (0° test), and pitch-up (15° test)), as indicated in figure 6. The nominal flight-path velocity was 27 m/sec and is approximately 70 percent of the flight stall speed for this type airplane. The dynamics of the swing system cause the airplane to pitch around its own center of gravity after cable separation. The resulting pitching velocities were 0.37 rad/sec for the pitch-down test, 0.35 rad/sec for the flat test, and 0.62 rad/sec for the pitch-up test. After cable separation, this pitching velocity results in less than 1° of pitch variation at impact.

Airplane Test Specimen

Airplane specimens used for the tests were twin-engine, general-aviation types having a nominal mass of 2700 kg, with a capacity for six occupants. (See fig. 7.) The three airplane specimens were stripped of all interior instruments, upholstery, panels, and floorboards such that the basic test specimens consisted of only the fuselage structural shell, wings with nacelle fairings, and landing gear (retracted during test). The mass and center of gravity of the empennage were simulated by two concentrated masses representing the fin-rudder and stabilizer-elevator combinations. The masses and center of gravities of the engines, propellers, spinners, ailerons, and flaps were also simulated by concentrated masses. The fuel cells were filled with colored water to simulate the fuel mass and to help identify any leaking fuel cells during the test. Spoilers were attached to the wings to minimize the aerodynamic lift.

The exterior and interior of the airplane specimens were painted to enhance the photographic contrast, and black lines were painted over rivet lines to delineate the underlying structure.

The three airplane specimens were similar except in the interior. (See figs. 8 and 9.) The first-passenger dummy, with a mass of 88 kg, the seat, and the five-point harness restraint system were the same for all three specimens. The pilot dummy, with a mass of 64 kg, and the seat were the same for all three specimens; however, the pilot restraint system for the flat test consisted of a lap belt and a single shoulder strap over the right shoulder, whereas the pitch-down and pitch-up tests had lap belts and single shoulder straps over the left shoulders. The copilot (82 kg) and second-passenger dummies (88 kg) in the pitch-down test had lap belt restraints only. The copilot dummies (66 kg), the seats, and the harness systems were the same for the flat and pitch-up tests; the copilots were restrained with lap belts and single shoulder straps over the right shoulders. The second passenger, with a mass of 88 kg, was restrained with a standard lap belt and a single shoulder strap over the left shoulder for the flat test. The pitch-up test did not have a dummy and seat in the second-passenger location, but they were simulated with lead masses and a simulated seat frame, at a combined mass of 91 kg. In all three specimens, the third and fourth passengers were simulated with a balance distribution of lead masses, batteries, pyrotechnic programmers, and instrumentation boxes (ref. 7).

INSTRUMENTATION

Onboard instrumentation for obtaining data pertaining to the dynamic behavior of the airplane structure, seats, and dummies consisted of ac accelerometers and high-speed motion-picture cameras. External photographic coverage of the crash sequence was provided by tracking and fixed motion-picture cameras located to the port side of the test specimen and by fixed motion-picture cameras in front of and overhead of the test specimen (fig. 2). To obtain the horizontal velocity of the test specimen at impact, a Doppler radar unit was placed on the impact surface, approximately 60 m aft of the impact point, and the signal recorded on one channel of an FM tape recorder.

The accelerometer locations common to all three airplanes are shown in figure 10. The accelerometers were oriented along the normal (Z), longitudinal (X), and transverse (Y) axes, as shown in figure 5. Each location is designated by its grid coordinates as follows: the first number indicates the longitudinal coordinate; the first letter indicates the normal coordinate (floor to roof); the second number indicates the transverse coordinate; the second letter indicates the accelerometer orientation with respect to the airplane body-axis system. For example, the normal accelerometer location on the floor beam nearest the nose is designated 2B9N. The normal, longitudinal, and transverse orientations are designated as N, L, and T, respectively. The accelerometer locations and the orientations in the dummies are given in the table in figure 10. The orientations of the accelerometers are given in the dummy's body-axis system, and the locations are given in the airplane grid coordinate system.

Data signals were transmitted through an umbilical cable, to a junction box on top of the gantry, and from there, through hard wire, to the control room, where they were recorded on FM tape recorders (fig. 2). To correlate the data signals on the FM recorders with the external motion-picture camera data, a time code was recorded simultaneously on the magnetic tape and on the film. There was also a time pulse generator onboard the airplane for the onboard cameras.

The accelerometers and data-reduction techniques are described in reference 6. The output of the piezoelectric accelerometers exhibited various degrees of zero shift with increasing time. This problem was compounded by the multiplicity of pulses to which each accelerometer was subjected during the tests. As a result, there is some unknown error in the absolute value of accelerations recorded after the first pulse. The first acceleration pulses are believed to be accurate within 10g. The first distinct peaks are labeled on the data plots presented in this report.

RESULTS AND DISCUSSION

Crash Dynamics

A sequence of crash-test photographs for each airplane test specimen is shown in figure 11 at 0.05-sec intervals.

The photographic sequence for the pitch-down test (fig. 11(a)) illustrates the crash dynamics of the test specimen, starting at 0.015 sec after initial ground contact at -12° pitch, with velocity components of 26 m/sec horizontal and 7.5 m/sec vertical relative to the impact surface (fig. 6). Initial ground contact is followed by the crushing of the nose and the downward rotation of the aft end of the fuselage. A second impact occurs as the specimen slams down at about 0.165 sec imparting additional impact loads normal to the fuselage floor. This impact causes the fuselage to expand in the transverse direction, ripping open the fuselage along the windows and breaking (rivet shear) the fuselage overhead at the frame behind the pilot about 0.215 sec into the crash.

The photographic sequence for the flat test (fig. 11(b)) indicates that the airplane fuselage did not rotate during this crash but simply slammed in at its initial 4° pitch attitude, with velocity components of 26 m/sec horizontal and 7 m/sec vertical relative to the impact surface (fig. 6). The point of impact was near the door just aft of the third and fourth passenger locations where the maximum damage occurred in the fuselage floor.

The photographic sequence for the pitch-up test (fig. 11(c)) illustrates the test specimen contacting the ground on the lower aft section of the fuselage at 14° pitch, with velocity components of 26 m/sec horizontal and 7.5 m/sec vertical relative to the impact surface (fig. 6). During the impact, the aft section of the fuselage experienced considerable structural damage, although the downward rotation of the nose of the specimen was less severe than the downward rotation of the aft end of the fuselage in the pitch-down test. During slide-out, the specimen rocked forward, with a minor second impact occurring at 0.100 sec, and continued to rock forward until it was sliding on the forward bottom section of the fuselage. It eventually settled back onto the underside of the cabin compartment.

Assessment of Exterior Damage

A postcrash comparison of the exterior damage sustained by each of the three test specimens is shown in figures 12 to 15. The cables and straps noted around the nose of each specimen were part of the arresting system used to stop the airplane forward motion. The livable cabin volume (i.e., a volume which remains sufficient in size to maintain space between the occupant and the structure) was maintained throughout the crash in each of the three test specimens.

Pitch-down test.- The photograph of the test specimen for the pitch-down test (fig. 12(a)) shows extensive buckling damage to the lower part of the fuselage from the nose to the fire wall, which was the primary impact area. The separation of the skin at the lower edge of the windows on the port side was caused by rivet-shear failure during the slam down or second impact. The window breakage also occurred at this time; however, the pilot's head impacting the window 0.165 sec into the crash (fig. 11(a)) may have contributed to side-window breakage.

A close-up view of the window section of the specimen is presented in figure 13(a). The separation in the fuselage at the frame just aft of the pilot is directly over the main wing spar that passes through the fuselage. This separation occurred as the specimen tail reached its lowest position during downward rotation, which caused the top of the fuselage to go into tensile loading, thus shearing the rivets that attach the skin to the frame.

Figure 13(b) shows the rivet-shear failure under the windows on the starboard side of the fuselage. This type failure also occurred in the lower section of the fuselage on the starboard side at the frame forming the leading edge of the door on the opposite side. The greatest rivet-shear damage occurred on the port side of the fuselage (fig. 11(a) and fig. 13).

The large door opening on the port side breaks the continuity of the fuselage structure to make it more susceptible to structural buckling during the crash. During the second impact, this port-side weakness led to tensile loading of the starboard side, which sheared the rivets that fasten the skin to the frame (fig. 13(b)). The small yaw angle of 1° at initial ground contack may have been a contributing factor in the more severe damage on the port side. The door opened on second impact and did not contribute to the strength of the structure on that side of the fuselage.

Flat test.- The photograph of the test specimen for the flat test (fig. 12(b)) shows only skin wrinkles in the forward section of the airplane specimen. The initial contact of the fuselage with the ground was in the vicinity of the door. The transverse expansion of the fuselage caused separation of the skin under the windows, as in the pitch-down test, but the degree of separation was less. More severe lower fuselage damage was sustained in the vicinity of the third window and extended rearward through the baggage compartment aft of the door (fig. 14). Separation of the skin along the bottom of the windows on the starboard side of the fuselage is shown in figure 14(a). As in the pitch-down test, the port side sustained more rivet-shear damage along the windows than the starboard side, thus supporting the conclusion that the door opening weakened the fuselage on the port side. In this test, the door opened immediately after the first ground contact.

Pitch-up test.- The photograph of the test specimen for the pitch-up test (fig. 12(c)) shows very little damage to the port side of the specimen. Small wrinkles or buckling can be noted at the nose near the fire wall and aft of the door. Separation of the skin under the windows due to rivet shear is shown in figure 15(a), but was not nearly as severe as in the pitch-down and flat tests. The primary impact occurred along the aft fuselage section at the baggage compartment. The separation and buckling of the skin on the bottom of the fuselage at the frame forming the aft edge of the door was a result of the tensile loading in the bottom of the specimen as the aft end of the specimen contacted the ground. Separation of the skin on the starboard side of the specimen is shown in figure 15(b). The door opened immediately after initial ground contact as it did in the flat test.

Assessment of Interior Damage

The postcrash interior damage sustained by each of the airplane specimens is presented with photographs in figures 16, 17, and 18. These photographs and motion pictures show that the livable volume was maintained in the passenger and crew cabin sections. There was some intrusion of the specimen floor structure into the cabin in all three tests, and each specimen showed evidence of side-wall expansion during the tests.

Pitch-down test.- The photograph from the pitch-down test (fig. 16(a)) was taken from the aft end of the fuselage looking forward. The intrusion of the floor structure into the cabin is shown by the outward rotated position of the seats. Because of the circular shape of the bottom of the fuselage, the out-

board floor structures were bent down around the two longitudinal floor beams which made first ground contact. Consequently the seats, dummies, and all items outboard of the floor beams rotated outward.

This rotation, together with the counterclockwise rotation of the pilot's body around the restraint strap crossing the left shoulder (fig. 9(a)), was responsible for the pilot's head impacting the side window, contributing to window breakage. The buckles in the door frame resulted from the transverse expansion of the fuselage during impact. The photograph taken from the pilot's position looking rearward (fig. 16(b)) shows only small buckles in the cross members between the floor beams and very little evidence of any damage in the aft section of the fuselage due to impact.

Flat test.- The photograph from the flat test (fig. 17(a)) was taken from the aft end of the fuselage looking forward. The outboard rotated position of the seats is much more pronounced than in the pitch-down test. The floor structure was pushed upward, with buckling and rivet-shear failures throughout the floor area. The longitudinal floor beams, which are fabricated from flat stock and extrusions riveted together, separated along the rivet lines. The photograph taken looking through the doorway at the structural damage in the vicinity of the fuselage where first ground contact occurred (fig. 17(b)) indicated that the floor structural damage was extensive and included buckling, rivet-shear failure, breaking, and tearing of the structure. This damage area extended back to the frame of the baggage compartment farthest aft, as shown in figure 17(c). The photograph (fig. 17(d)) shows a break in the main wing spar near the center of the fuselage.

Pitch-up test.- The photograph from the pitch-up test that was taken from the aft end of the fuselage looking forward (fig. 18(a)) shows the same type of outboard-rotated position of the seats as previously noted. The second-passenger dummy used in the previous tests was simulated with lead masses in this test. Although the external pictures (fig. 15) indicated less structural damage than in the pitch-down and flat tests, the pictures of the internal structure in the vicinity of the door and baggage compartment (fig. 18(b)) show damage similar to the flat test. The floor damage in the passenger section of the fuselage (fig. 18(c)) shows some structural buckling, rivet shear, and total failures of the cross members between the longitudinal beam, but little damage to the beams themselves.

Acceleration Histories

The accelerometer locations common to all three test specimens are presented in figure 10, and the associated acceleration history traces are given in figures 19, 20, 21, and 22. Each figure presents the coordinates of accelerometer locations with respect to the airplane structure for each of the acceleration traces presented.

The analysis of the acceleration traces included time-event correlation with the corresponding crash scene from the motion-picture film. The acceleration traces were examined to determine the first major impact acceleration

peaks on the fuselage structure at the time the structural element on which the accelerometers were mounted made ground contact. These acceleration peaks are labeled on the acceleration traces presented in this report and are the same acceleration peaks referred to in the instrumentation section, which are believed to be accurate. Accelerations experienced prior to these peaks are effects of loads and structural vibrations that are transmitted through the airplane structure from impact pulses applied to other structural elements. These types of accelerations do not result in significant structural deformation. There are no peaks labeled on some traces because the first major impact acceleration peaks could not be identified. The least-squares fit of the acceleration time histories filters out the high-frequency accelerations that result from local structural vibrations. Some lower frequency vibratory accelerations are still evident in all of the time histories, however.

The common accelerometer data are presented and discussed for floor-beam normal accelerations, floor-beam longitudinal accelerations, floor and roof accelerations, and accelerations at seat legs and in the dummy. The data plots are grouped in normal and longitudinal orientations and include superimposed timed events obtained from photographic data film for correlation and interpretation.

Floor-Beam Normal Accelerations

Six normal-acceleration history traces along the floor beam of each test specimen are presented in figure 19. The accelerometers are located at major structural frames in the nose of the airplane and in the passenger compartment.

Pitch-down test.- The pitch-down test specimen made first ground contact in a -12° pitch attitude such that the first fuselage frame (2B9N) of figure 19(a) responded to the impact first, followed by the impact of consecutive frames back to the fire wall (8B9N). The acceleration histories show that the application of the major impact acceleration at the first frame peaked at 0.016 sec after ground contact, with a magnitude of -110g. The acceleration of the floor beam at the fire wall peaked at 0.019 sec, with a magnitude of -40g. The main spar contacted the ground at about 0.05 sec into the impact. During this time, the specimen continued to pitch to an attitude of -9°. The main spar acted as a fulcrum when it contacted the ground. This caused the angular velocity of the passenger compartment behind the spar to increase and the nose of the specimen to rotate off the ground, thus relieving all direct loadings in the nose section. The intensity of the accelerations decreased from -110g to -40g as the ground contact moved rearward to the spar. The floor from the spar (frame coordinate 13) through the third-passenger location (frame coordinate 19) was in ground contact within 0.08 sec after initial ground contact. During this time period, the spar buckled near the center of the cabin as the wing twisted and rotated down.

All wing dihedral was lost at 0.093 sec into the impact as the wing tips contacted the ground. About the same time, the fuselage started transverse expansion, causing rivet-shear failure along the windows at 0.11 sec. Further

pitching of the specimen continued until the aft end of the specimen, which normally has a 15° upward slope of the lower surface, came in contact with the ground, causing the roof of the specimen to separate (rivet-shear failure) at 0.177 sec after initial ground contact. All floor-beam accelerometers showed negative accelerations (stopping force) with ground contact, followed by positive accelerations as the nose lifted off the ground. Generally, the accelerations decrease progressively along the floor beam, from a maximum of -110g at the first frame in the nose (2B9N) to a minimum of -20g at the last frame instrumented (19B9N).

Flat test.- The flat-test specimen made first ground contact in a 4° pitch attitude, which resulted in initial ground contact at grid coordinate 21. The accelerometer at 19B9N (see fig. 19(b)) responded on initial ground contact. The specimen pitch attitude changed less than 1° during impact. Loads were progressively applied to the floor beams such that the fire wall (8B9N) was the last frame to contact the ground at 0.032 sec after initial ground contact. Very high accelerations were experienced in the passenger compartment aft of the main spar, with the greatest acceleration of -150g occurring in the third- and fourth-passenger location. These passenger-compartment accelerations were considerably higher for the flat specimen (-150g to -50g) than for the pitch-down specimen (-80g to -20g). The accelerations at the fire wall (8B9N) were very small. The accelerations at the first frame (2B9N) and second frame (5B9N) in the nose of the airplane were transmitted through the floor beam and attached structure since those two frames did not contact the ground during impact. The intensity of the first peaks exhibited the same trend but in the reverse direction as that in the pitch-down test (i.e., the intensity decreased as the ground contact moved forward). Maximum fuselage expansion occurred at 0.069 sec when all vertical velocity of the structure had ceased. There are no indications in the acceleration data of the main wing spar breaking (see fig. 17(d)), even though there was complete failure in the upper flange of the spar.

Pitch-up test.- The pitch-up test specimen made first ground contact along the slope of the lower surface of the tail section. The frame at grid coordinate 24 (fig. 19(c)) was extensively damaged on initial ground contact, and it took about 0.03 sec for the ground contact to move forward in the passenger compartment, when there was a major response at accelerometer 19B9N. The accelerations at this frame were very high (-200g), but as the ground contact moved further into the compartment, the accelerations at the succeeding frames were much lower (-50g to -20g) and of about the same magnitude as those of the flat test. It may be noted that the accelerations at the frames in the nose section (2B9N, 5B9N, and 8B9N) responded in the positive direction before the main spar contacted the ground at 0.067 sec into the impact. The accelerations of 35g, 20g, and 10g at frames 2B9N, 5B9N, and 8B9N, respectively, indicate a very high downward pitching rate as a result of the initial high nose-ground contact of 14° pitch. After the main spar contacted the ground, these same forward frames showed negative accelerations due to ground contact. By the time the wing tips made ground contact, the nose frames were already in ground contact, and the airplane continued to rock forward until only the nose section was in ground contact. Thereafter, all accelerations were very low as the airplane rocked back onto the bottom of the fuselage.

Floor-Beam Longitudinal Accelerations

Six longitudinal accelerometer traces along the floor beam are presented in figure 20 for each test specimen. The accelerometers are located at major structural frames in the nose of the specimen and in the passenger compartment. These accelerometers were mounted at the same locations as the normal accelerometers presented in the previous section.

Pitch-down test.- Figure 20(a) shows the response of the longitudinal accelerometers to impact for the pitch-down test. The magnitude of accelerations in the nose (2B9L to 8B9L) was very low during the deformation of the nose structure, which ended at about 0.02 sec into the impact. The later peaks were associated with the rebound of the nose section and the acceleration transmitted through the structure. Behind the main spar, structural deformation was felt over a much longer time since ground contact at 19B9L started about 0.08 sec after initial ground contact and continued for a period of 0.065 sec, or until maximum fuselage expansion at about 0.145 sec. The longitudinal acceleration traces do not show definite indication of specific structural failures.

Flat test.- Figure 20(b) shows the longitudinal acceleration histories for the flat test. The passenger-compartment accelerations indicate the effect of the 4° pitch attitude at initial impact by the slight time difference as the ground contact moves forward from 19B9L to 8B9L. The magnitudes of the accelerations aft of the main spar were nearly the same. The acceleration at 8B9L was smaller, and since this was the last frame to contact the ground, the very low accelerations at frames 5B9L and 2B9L were transmitted through the floor beams and associated structure. The longitudinal accelerations in the passenger compartment were considerably higher for the flat specimen than those for the pitch-down specimen.

Pitch-up test.- Figure 20(c) shows the longitudinal acceleration histories for the pitch-up test. The last frame in this figure is noted as 20B9L, instead of 19B9L as in figures 20(a) and 20(b). Since these frames are close together and are alike in structural features, the accelerations should be comparable. The lack of a definite pattern for the accelerations appears to be the result of the rocking motion of the airplane during impact. In general, the magnitude of these accelerations appears to fall between those for the pitch-down and flat tests.

Floor and Roof Accelerations

Accelerations on the floor (other than the floor beam) and along the roof are presented in figure 21 in the normal direction and in figure 22 in the longitudinal direction. The accelerometers at frames 11B8 and 13B8 were mounted on the aluminum floor boards between the pilot's fore and aft seat legs. As a result of this mounting, the acceleration traces show an oscillatory behavior that is typical of a local vibration. The large acceleration peaks are a result of the impact superimposed on the oscillatory traces. The window side

accelerations at 15B8 and 17B8 generally exhibited lower magnitudes in both the normal and longitudinal directions than their counterparts on the floor beam.

The accelerations at the roof (5E9 and 14G9) and at the tail (35F9) were much lower than those on the floor. The oscillatory nature of the acceleration traces would be expected since the roof is less rigid than the floor. This behavior of the structure also makes it more difficult to identify the first major impact acceleration peaks. The reduced magnitudes of the accelerations were a result of the flexible nature of the fuselage, which allows the fuselage sides to expand outward during impact which caused the roof to decelerate over a longer time period.

Accelerations at Seat Legs and in Dummy

The normal and longitudinal accelerations on the floor at the first passenger's seat legs and in the pelvic region of the first-passenger dummy are given in figure 23. The accelerometers on the floor were oriented in the airplane coordinate system, and the accelerometers in the dummy were oriented in the dummy's coordinate system. Superimposed timed events obtained from photographic data film are also presented in figure 23.

Pitch-down test.- The normal and longitudinal acceleration histories at the seat legs and in the dummy are presented in figures 23(a) and 23(b), respectively, for the pitch-down test. After the main spar contacted the impact surface (see fig. 19(a)) at 0.05 sec, the floor beam under the dummy experienced normal accelerations of -80g and -30g at the seat front and back legs, respectively. The floor on the window side experienced normal accelerations of -30g and -25g at the seat front and back legs, respectively. The accelerations peaked at about 0.073 sec into the impact. The dummy started to sink into the seat and move forward into the five-point harness restraint system within 0.02 sec after initial ground contact. The dummy experienced only small accelerations as he sank into the seat. The harness system began to tighten at about 0.08 sec into the impact, and the dummy's downward and forward motion was stopped at about 0.114 sec. The resulting delayed pelvic normal acceleration of -55g in the dummy is shown by the peak in the normal direction (fig. 23(a)) and to a greater extent in the longitudinal acceleration of -80g (fig. 23(b)) at 0.114 sec. The seat started to rotate outboard following the deformation of the floor structure at about 0.07 sec, and continued for 0.117 sec. The seat-leg and dummy accelerometers showed negligible accelerations after the seat stopped rotating.

Flat test.- The normal and longitudinal acceleration histories at the seat legs and in the dummy are presented in figures 23(c) and 23(d), respectively, for the flat test. Since the airplane contacted the impact surface at a 4° pitch attitude, the impact acceleration in the first-passenger dummy was felt before the main spar contacted the impact surface. The floor beam under the seat experienced normal accelerations of -80g and -50g at the seat back and front legs, respectively. The floor on the window side experienced normal acceleration of -50g and -35g at the seat back and front legs, respectively. The dummy experienced normal accelerations of -40g and 0.02 sec after those

on the floor, as compared with -55g for the pitch-down test, even though the accelerations on the floor were higher for the flat test. Unlike the pitch-down test, the dummy did not move forward into the restraint system but sank into the seat and rebounded upward into the shoulder straps. Most of the accelerations were felt by the dummy during the time the seat was rotating outboard.

Pitch-up test.- The normal and longitudinal accelerations at the seat legs and in the dummy are presented in figures 23(e) and 23(f), respectively, for the pitch-up test. The effect of the 14^{o} pitch-up angle at ground contact is shown by the greater acceleration at the back legs of the seat than at the front legs. The floor beam under the seat experienced normal accelerations of -50g and -20g at the back and front seat legs, respectively. The floor on the window side experienced normal accelerations of -40g and -20g at the back and front seat legs, respectively. The first-passenger dummy started to move down into the seat within 0.01 sec after ground contact on the aft lower surface of the airplane. The forward rocking motion of the fuselage caused the dummy to move backward into the seat at the same time that he moved down into the soft seat cushion and supporting diaphragm. At 0.053 sec after ground contact, the dummy stopped his downward motion. At the same time, the normal accelerations at the seat legs peaked (negative magnitude, fig. 23(e)). As the dummy's sinking motion stopped, the dummy started to submarine under the lap belt which was attached to the seat at the floor. At the same time, the seat started to rotate outboard, causing a positive response to the dummy's longitudinal accelerometer (fig. 23(f) and accelerometer 16C8L). The accelerometer was oriented along the longitudinal axis of the dummy (perpendicular to the spine); however, the submarining caused the accelerometer to rotate into an orientation almost parallel to the airplane normal axis (see fig. 24). Consequently, response of the longitudinal accelerometer was due to the stopping motion along the normal axis of the airplane. The acceleration of 30g peaked at about 0.065 sec into the impact. At 0.067 sec after ground contact, the airplane downward velocity was arrested, and rebound of the floor beams started as the airplane continued to rock forward. The reversal of direction caused positive normal acceleration peaks on the floor beam at the base of the seat. The seat continued to rotate outboard until 0.124 sec, after which time all accelerations were negligible.

Damage and Acceleration Evaluation

The significant normal acceleration peaks on the floor of the passenger compartment at the first passenger's seat legs and in the first passenger's pelvis are presented in table II and figure 25. The measured maximum normal acceleration peaks on the compartment floor were -80g, -150g, and -200g for the pitch-down, flat, and pitch-up test specimens, respectively. Table II shows that these maximum acceleration peaks did not generally occur at the same locations on the compartment floor or at the same seat-leg location. In the pitch-down test, both the passenger-compartment and seat-leg maximum acceleration peaks occurred at the seat front leg (15B9N) and had the same magnitude. For the flat and pitch-up tests, the maximum acceleration peaks on the floor occurred at the rear of the compartment near the fuselage door, and the maximum acceleration peaks at the first-passenger seat occurred at the rear seat legs. These differences in acceleration peaks between the seat legs and com-

partment floor (fig. 25) are caused by the combination of pitch attitude of the airplane at ground contact, the airplane structural deformation aft of the first-passenger seat, the dynamic reactions of the dummy in the seat, and the changing attitude of the airplane during impact. Because the kinetic energy at impact is the same for the three test specimens, the lower acceleration peaks at the seat legs can be mainly attributed to structural deformation aft of the seat. This is reflected in the lower values of first-passenger seat-leg accelerations (table II). The acceleration differences between the floor at the seat legs and those in the pelvic region of the first-passenger dummy can be as much as 40g.

The difference in physical damage to the passenger compartments that accompanied these accelerations is presented by the photographs in figure 25. The damage increased from the pitch-down to pitch-up tests. The peak accelerations in the pelvic region of the first-passenger dummy decreased from -55g, to -40g, to -30g for the pitch-down, flat, and pitch-up tests, respectively. As the fuselage structural damage increased, peak pelvic accelerations in the first-passenger dummy decreased.

CONCLUDING REMARKS

Three general-aviation airplane specimens were crash tested at the Langley impact dynamics research facility under controlled free-flight conditions. The nominal test parameters were ground-contact pitch angles of -15° (pitch-down), 0° (flat), and 15° (pitch-up); a flight-path angle of -15°; and a flight-path velocity of 27 m/sec. All other parameters were essentially the same for the three tests.

The livable volume in the airplane cockpits and passenger compartments was maintained in all three test specimens, although there was some intrusion of the specimen floor structures into the passenger compartments. The structure of the floor in the passenger compartments in the vicinity of the third window sustained considerable damage in the flat and pitch-up test specimens but only small buckles in the pitch-down test specimen. Each of the airplane test specimens sustained separation of the skin under the windows due to rivet-shear failure.

The magnitudes of the normal accelerations on the floor beams in the passenger compartment were considerably higher in the flat and pitch-up tests than in the pitch-down test. The highest accelerations occurred at the third window locations in the fuselage. Longitudinal accelerations on the floor beams were highest in the flat test and lowest in the pitch-down test.

The differences in acceleration peaks between the seat legs and the compartment floor are caused by the combination of pitch attitude of the airplane at ground contact, the airplane structural deformation aft of the first-passenger seat, the dynamic reactions of the dummy in the seat, and the changing attitude of the airplane during impact. These peak accelerations do not generally occur at the same locations on the compartment floor or at the same

seat-leg location. The peak accelerations in the pelvic region of the first-passenger dummy were -55g, -40g, and -30g for the pitch-down, flat, and pitch-up tests, respectively. The peak pelvic accelerations in the first-passenger dummy decreased as the fuselage structural damage on the floor increased. The first-passenger dummy moved forward into the five-point restraint system during initial impact in the pitch-down test. In the pitch-up test, the first-passenger dummy submarined under the lap belt as a result of the dummy sinking into the soft seat cushion and supporting diaphragm.

Langley Research Center
National Aeronautics and Space Administration
Hampton, VA 23665
October 9, 1979

REFERENCES

1. Preston, G. Merritt; and Moser, Jacob C.: Crash Loads. NACA Conference on Airplane Crash-Impact Loads, Crash Injuries and Principles of Seat Design for Crash Worthiness (Cleveland, Ohio), Apr. 1956, pp. 2-1 - 2-47.

2. Eiband, A. Martin; Simpkinson, Scott H.; and Black, Dugald O.: Accelerations and Passenger Harness Loads Measured in Full-Scale Light-Airplane Crashes. NACA TN 2991, 1953.

3. Pinkel, I. Irving; and Rosenberg, Edmund G.: Seat Design for Crash Worthiness. NACA Rept. 1332, 1957. (Supersedes NACA TN 3777.)

4. Thomson, Robert G.; and Goetz, Robert C.: NASA/FAA General Aviation Crash Dynamics Program - A Status Report. AIAA Paper 79-0780, Apr. 1979.

5. Alfaro-Bou, Emilio; and Vaughan, Victor L., Jr.: Light Airplane Crash Tests at Impact Velocities of 13 and 27 m/sec. NASA TP-1042, 1977.

6. Castle, Claude B.; and Alfaro-Bou, Emilio: Light Airplane Crash Tests at Three Flight-Path Angles. NASA TP-1210, 1978.

7. Castle, Claude B.; and Alfaro-Bou, Emilio: Light Airplane Crash Tests at Three Roll Angles. NASA TP-1477, 1979.

8. Vaughan, Victor L., Jr.; and Alfaro-Bou, Emilio: Impact Dynamic Research Facility for Full-Scale Aircraft Crash Testing. NASA TN D-8179, 1976.

TABLE I.- IMPACT PARAMETERS FOR TWIN-ENGINE AIRPLANE SPECIMENS

Flight-path angle, deg	Pitch angle, deg	Roll angle, deg	Yaw angle, deg	Angle of attack, deg	Velocity, m/sec	Source
-15	-15	0	0	0	13	Reference 5
[a]-15	-15	0	0	0	[b]27	References 5, 6, 7, and present paper
-30	-30	0	0	0	27	Reference 6
-45	-45	0	0	0	27	Reference 6
[a]-15	0	0	0	15	27	Present paper
[a]-15	15	0	0	30	27	Present paper
-15	-15	-15	0	0	27	Reference 7
-15	-15	-30	0	0	27	Reference 7

[a]Specifically discussed in present paper.
[b]Maximum velocity for free fall due to height limitation.

TABLE II.- ACCELERATION PEAKS ON THE PASSENGER COMPARTMENT FLOOR AND AT SEAT LEGS FOR THE THREE TESTS

Test	Acceleration peaks, g, at frame -			
	15B9N	17B9N	19B9N	Pelvis
Pitch-down	-80	-30	-20	-55
Flat	-50	-80	-150	-40
Pitch-up	-20	-50	-200	-30

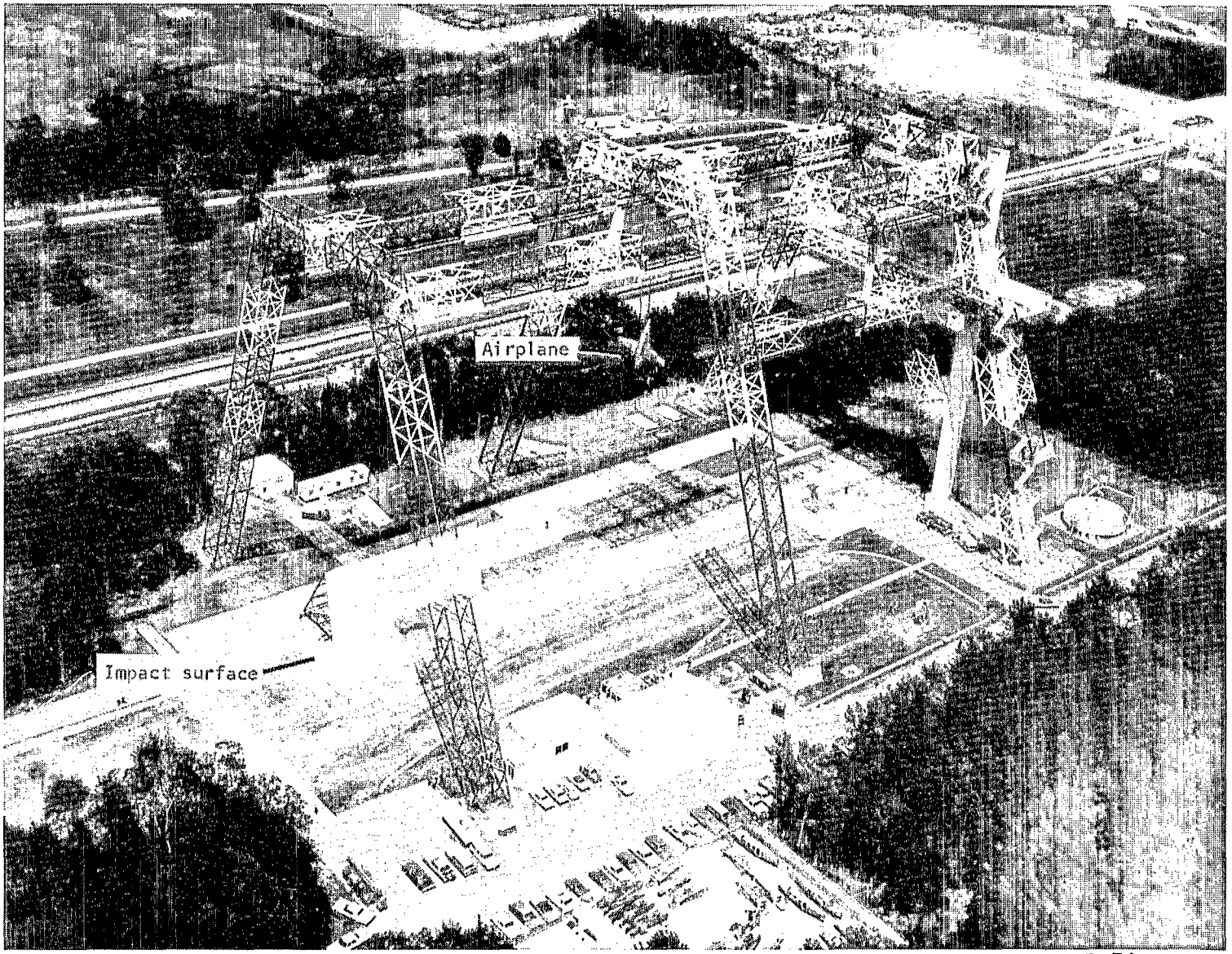

L-74-2505.5

Figure 1.- Langley impact dynamics research facility.

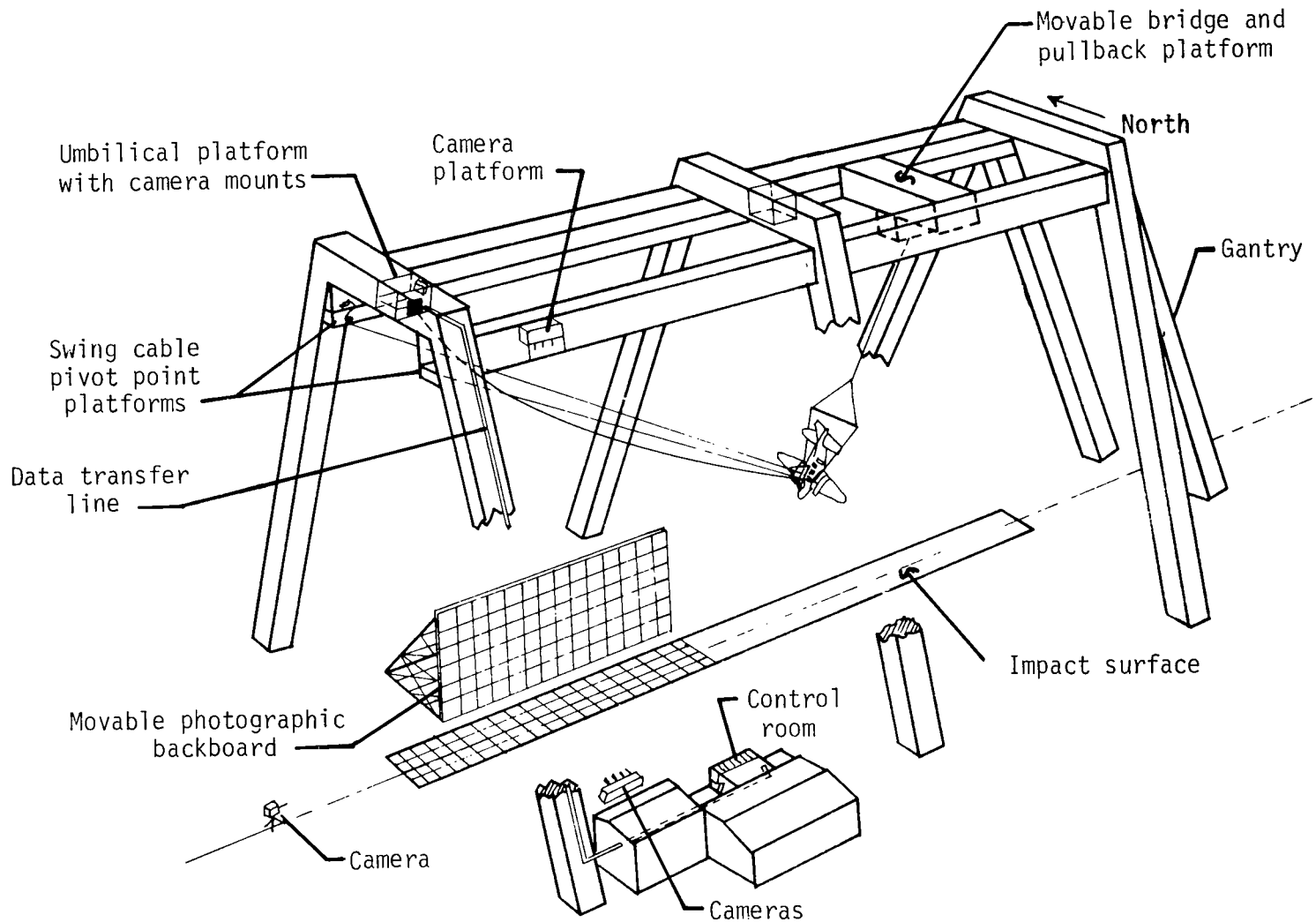

Figure 2.- Diagram of Langley impact dynamics research facility.

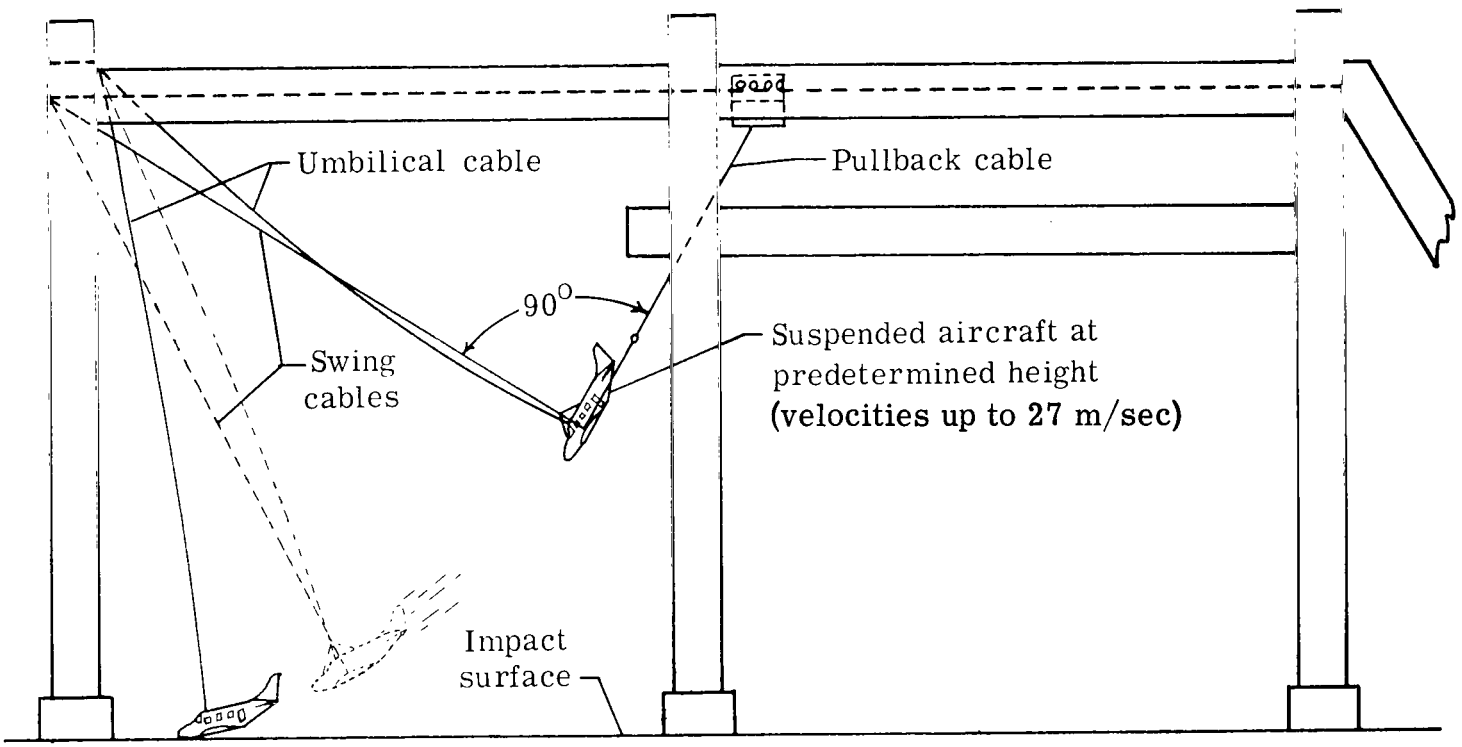

Figure 3.- Full-scale airplane crash-test technique.

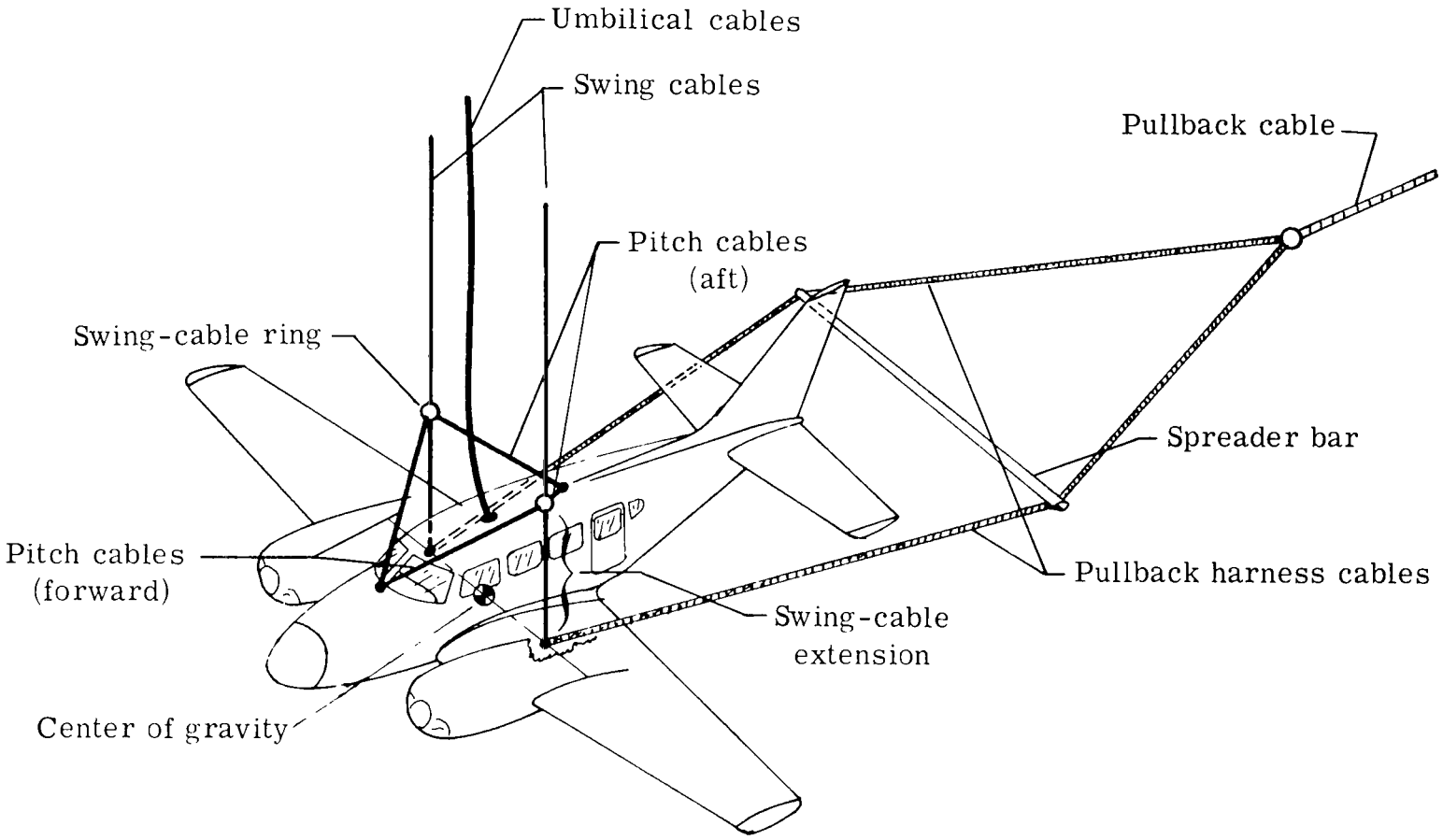

Figure 4.- Aircraft suspension system.

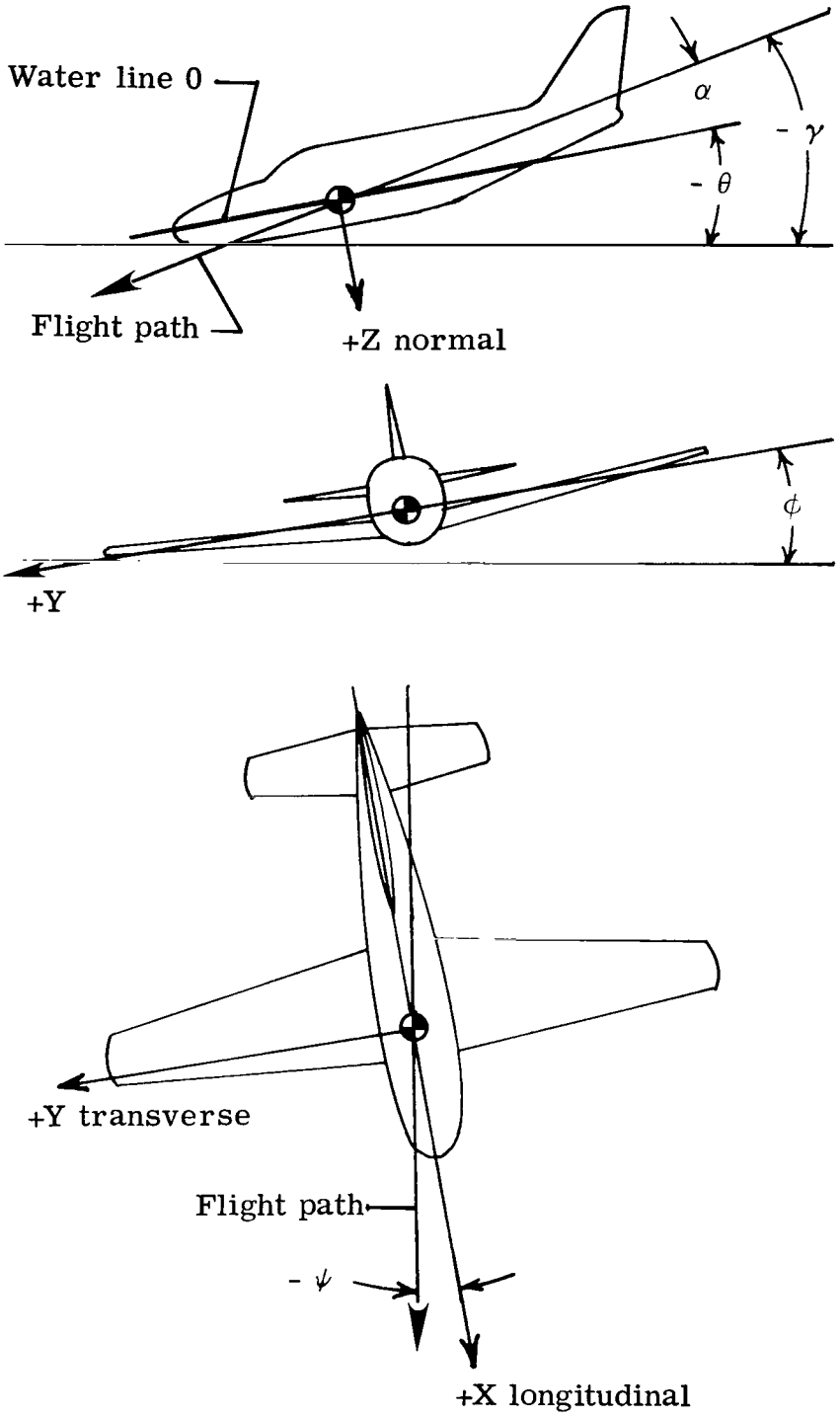

γ Flight-path angle
α Angle of attack
θ Pitch angle,
$\theta = \gamma + \alpha$

ϕ Roll angle

ψ Yaw angle

Figure 5.- Sketches identifying flight path, crash attitudes, axes, and force directions.

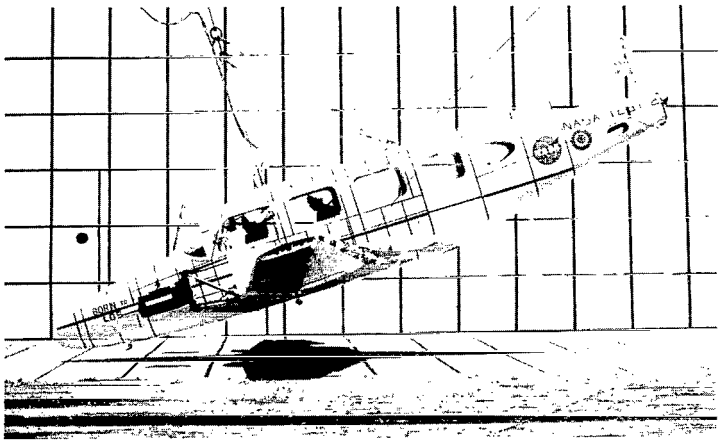

(a) Pitch-down test.

Flight-path angle, γ	-16°
Angle of attack, α	4°
Pitch angle, θ	-12°
Roll angle, ϕ	0°
Yaw angle, ψ	1°
Flight-path velocity	27 m/sec
Pitching velocity	0.37 rad/sec

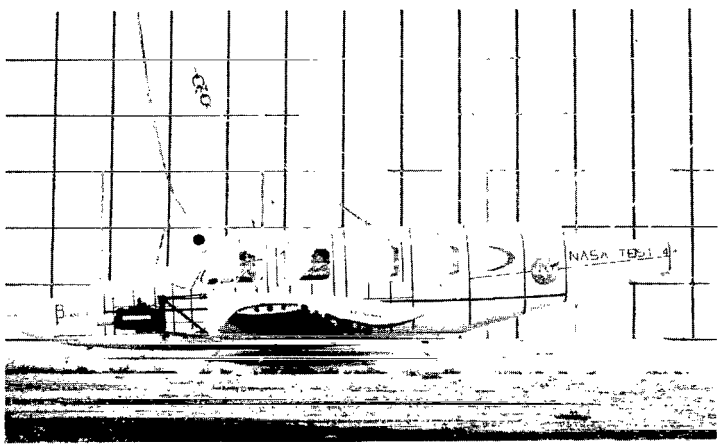

(b) Flat test.

Flight-path angle, γ	-15°
Angle of attack, α	19°
Pitch angle, θ	4°
Roll angle, ϕ	0°
Yaw angle, ψ	-1°
Flight-path velocity	27 m/sec
Pitching velocity	0.35 rad/sec

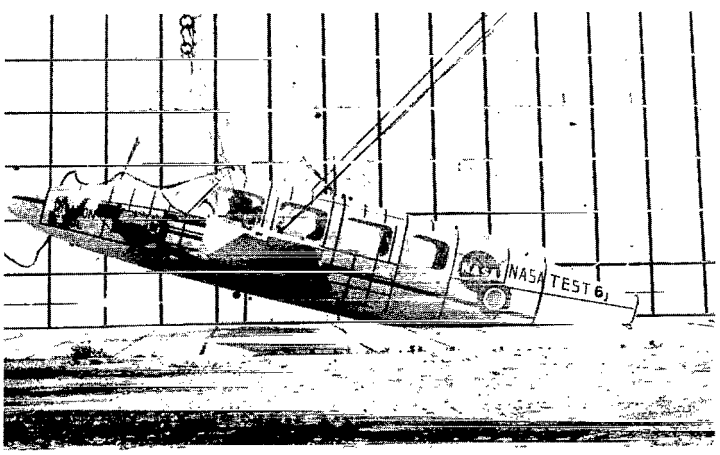

(c) Pitch-up test.

Flight-path angle, γ	-16°
Angle of attack, α	30°
Pitch angle, θ	14°
Roll angle, ϕ	1°
Yaw angle, ψ	0°
Flight-path velocity	27 m/sec
Pitching velocity	0.62 rad/sec

L-79-302

Figure 6.- Airplane pretest photographs and crash-test attitudes and parameters.

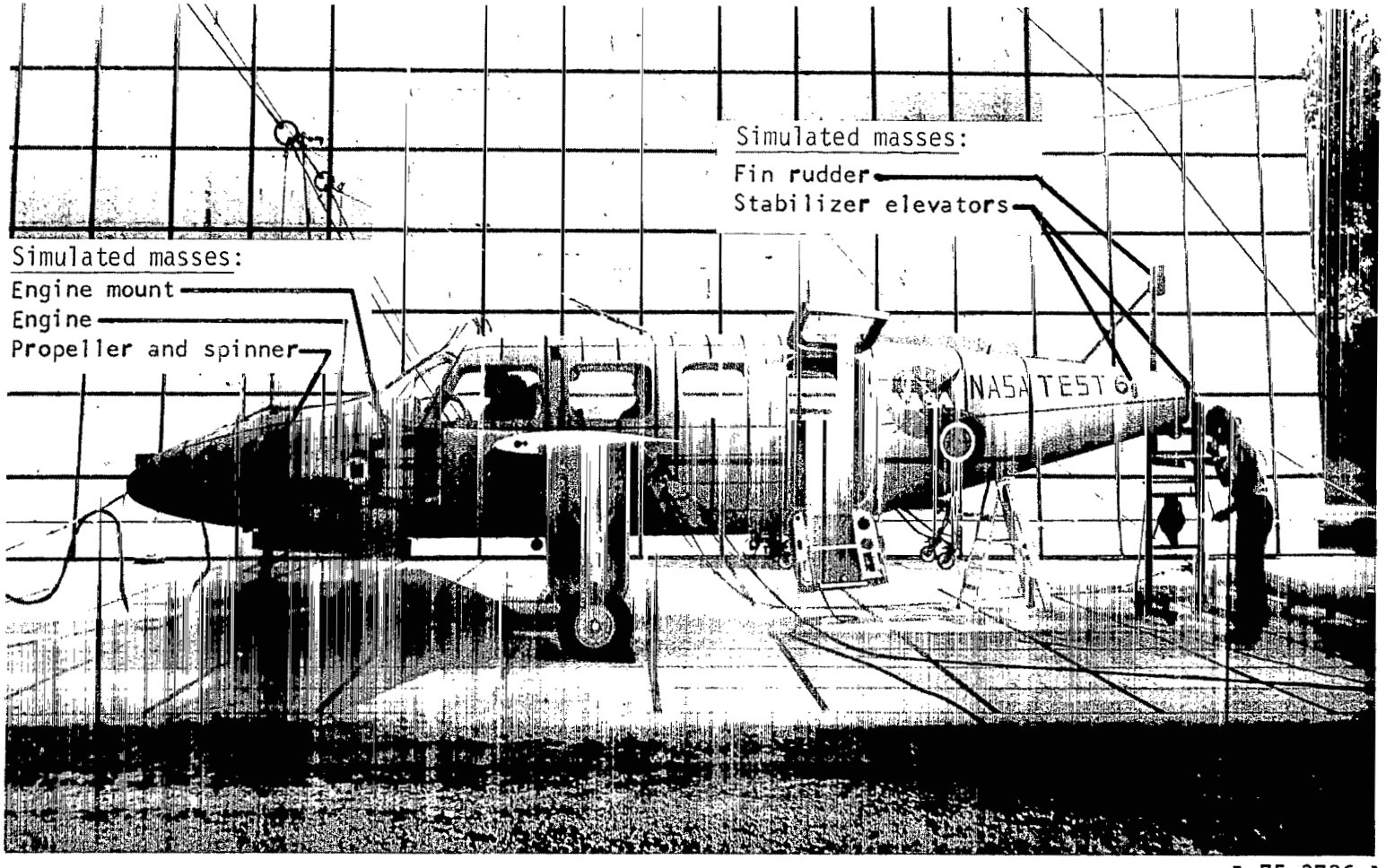

L-75-3736.1

Figure 7.- Typical airplane test specimen in crash-test preparation.

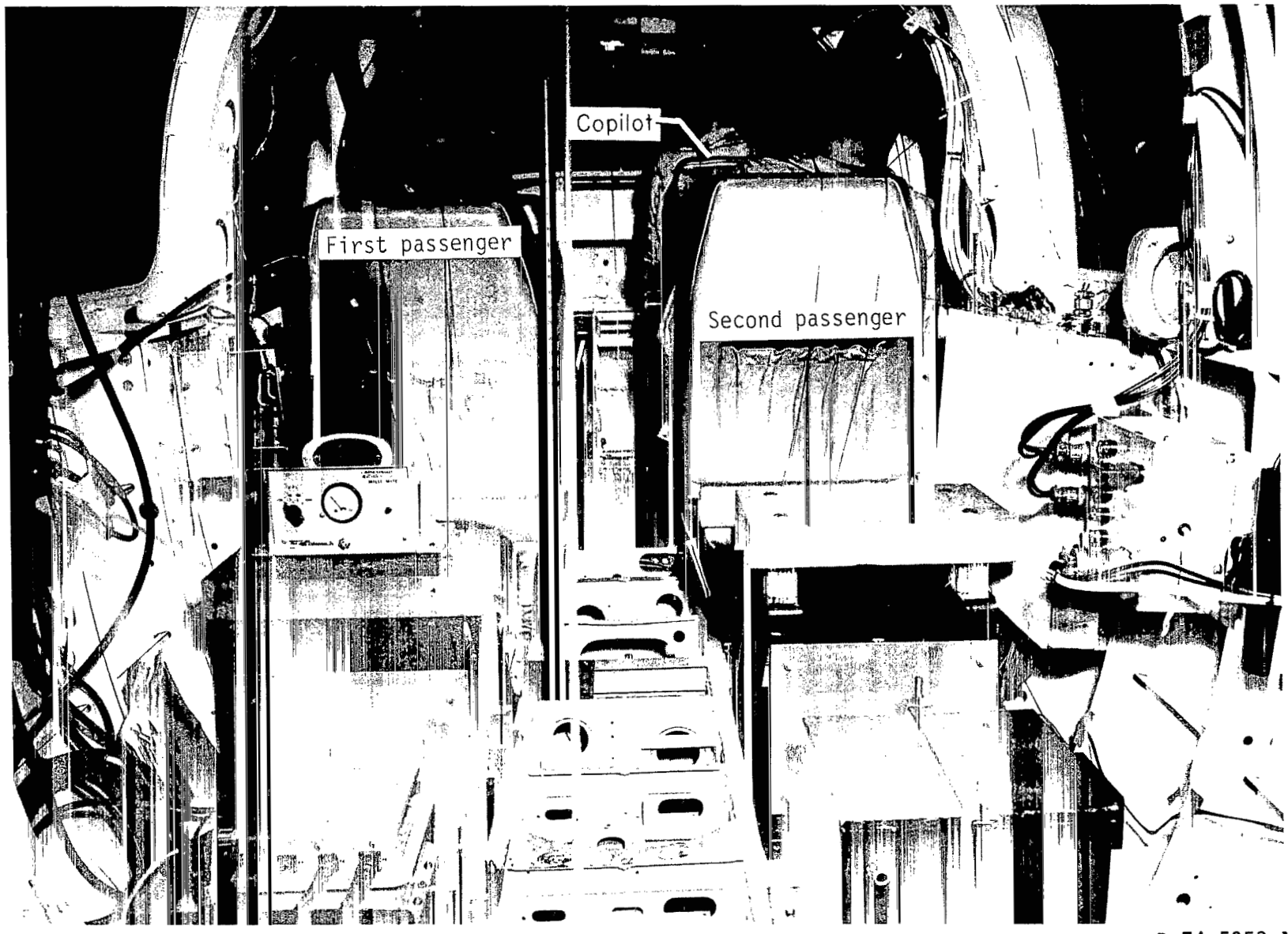

Figure 8.- General configuration of airplane interior before tests.

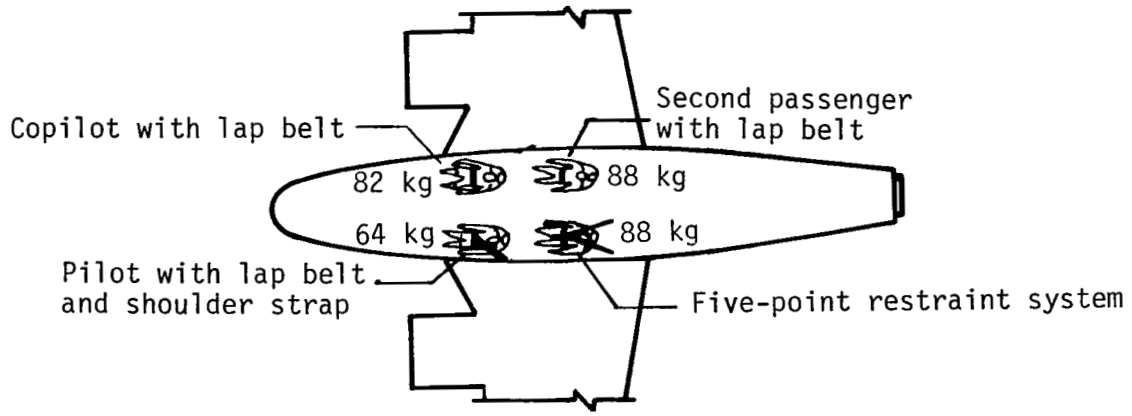

(a) Pitch-down test specimen.

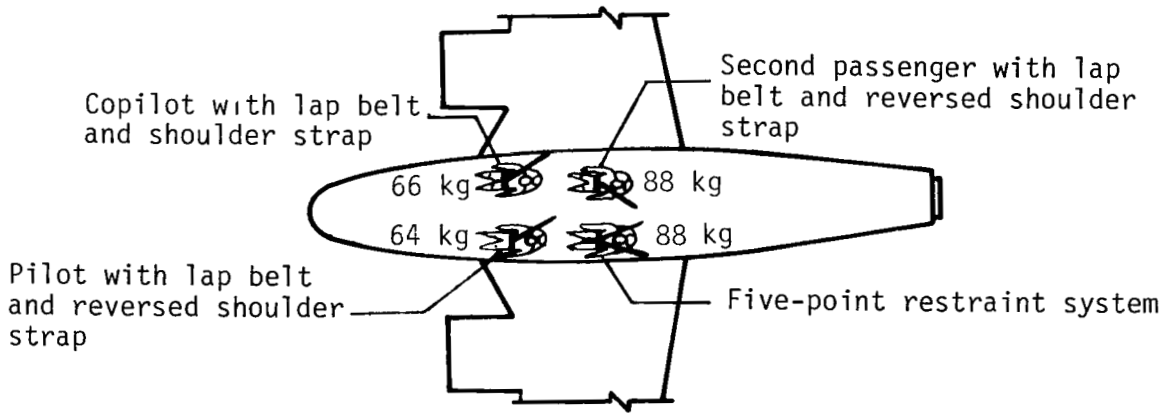

(b) Flat test specimen.

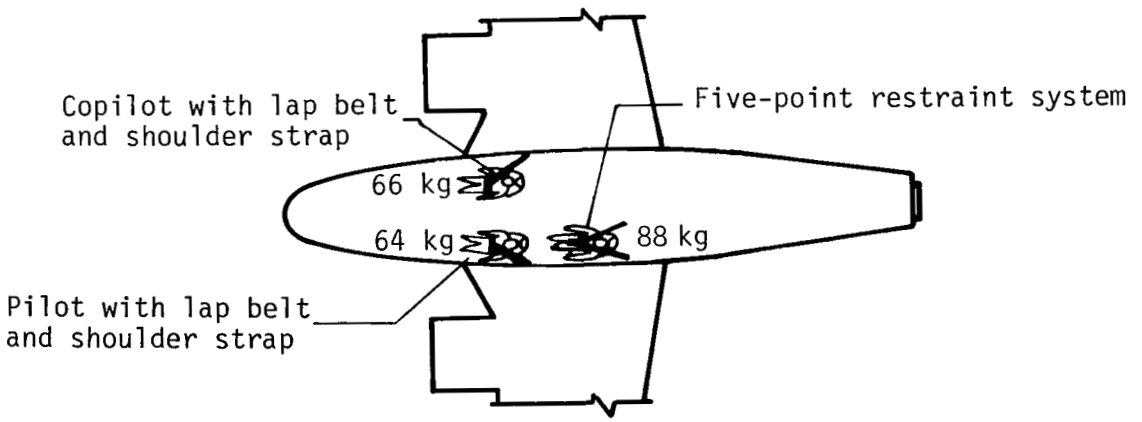

(c) Pitch-up test specimen.

Figure 9.- Arrangement of seats, dummies, and restraint systems for various test specimens.

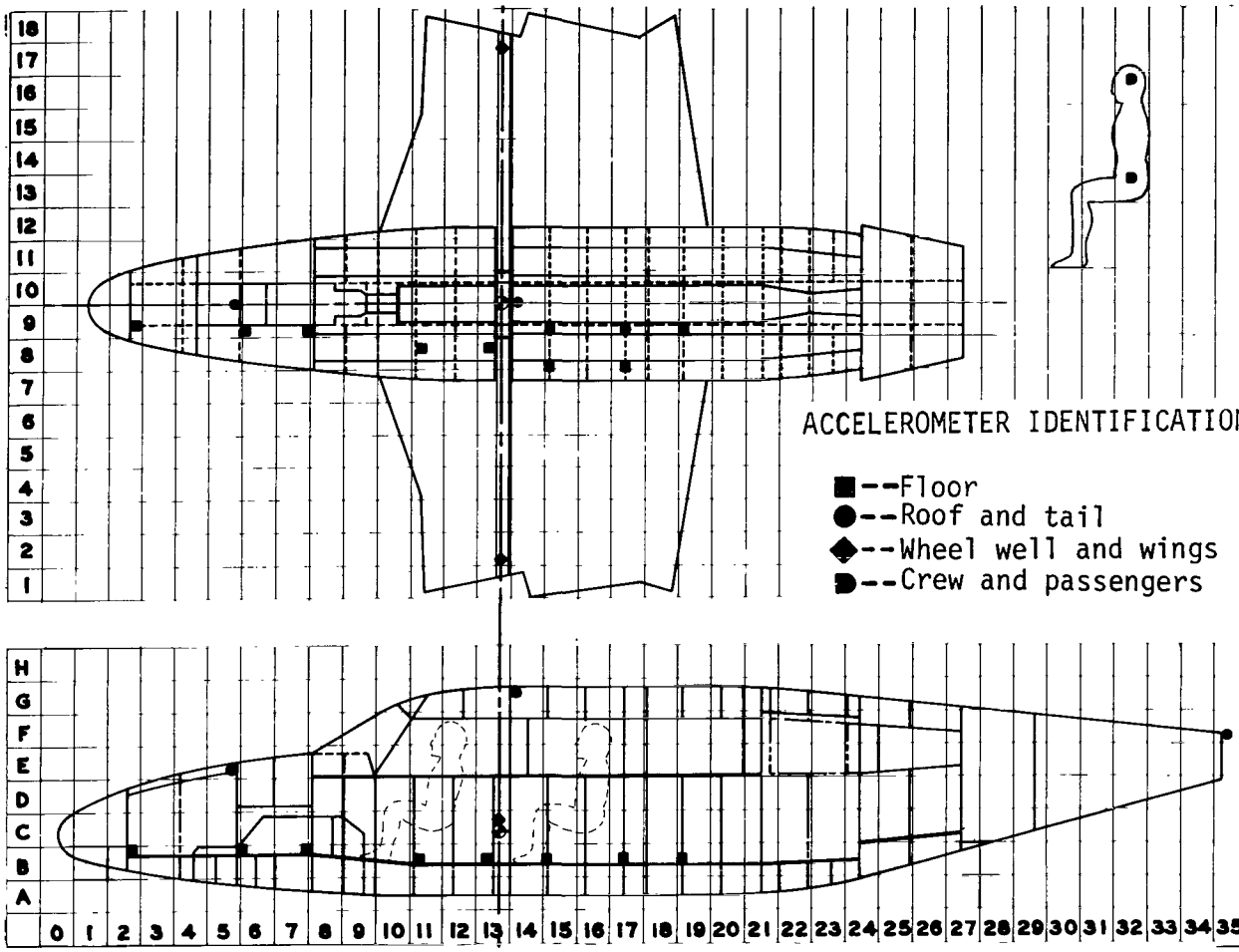

Accelerometers in dummies

Pilot, pelvic, normal*	12C8N
Pilot, pelvic, longitudinal**	12C8L
Pilot, head, normal	12F8N
Pilot, head, longitudinal	12F8L
1st passenger, pelvic, normal	16C8N
1st passenger, pelvic, longitudinal	16C8L
1st passenger, head, normal	16F8N
1st passenger, head, longitudinal	16F8L

*Along the spine

**Perpendicular to spine

Figure 10.- Diagram of accelerometer common to all three test specimens.

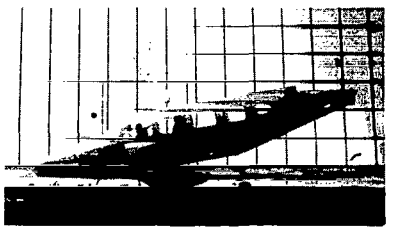

Time = 0.015 sec

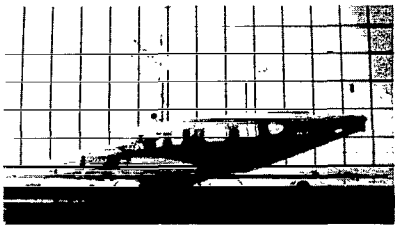

Time = 0.065 sec

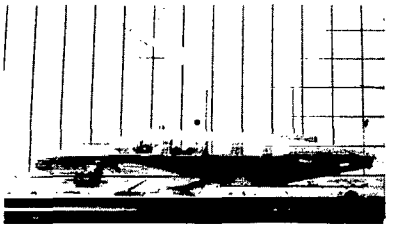

Time = 0.115 sec

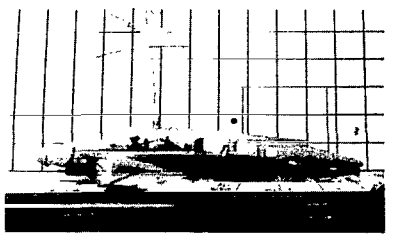

Time = 0.165 sec

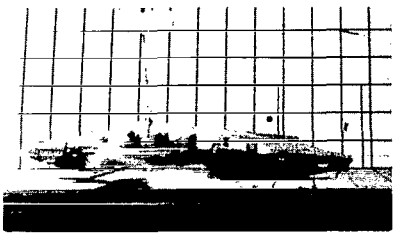

Time = 0.215 sec

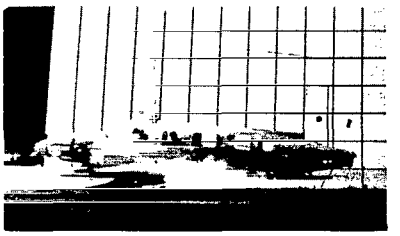

Time = 0.265 sec

(a) Pitch-down test.

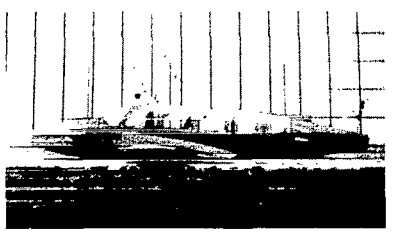

Time = 0.030 sec

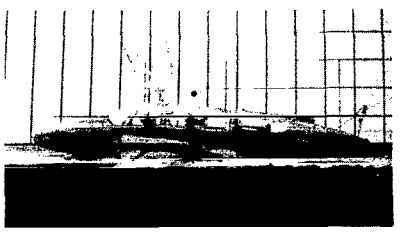

Time = 0.080 sec

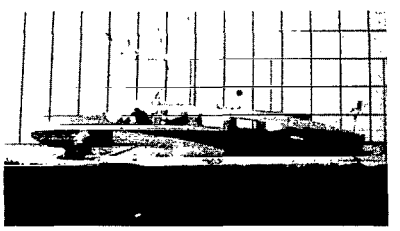

Time = 0.130 sec

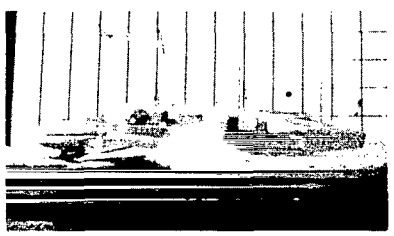

Time = 0.180 sec

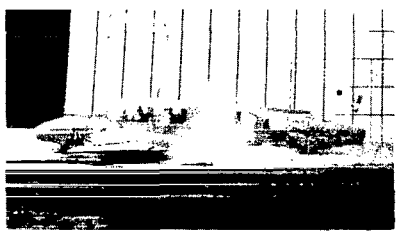

Time = 0.230 sec

Time = 0.280 sec

(b) Flat test.

L-79-303

Figure 11.- Crash sequence photographs for each of three tests.

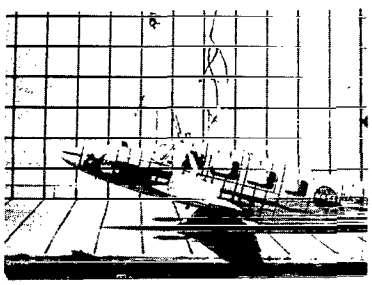

Time = 0.000 sec

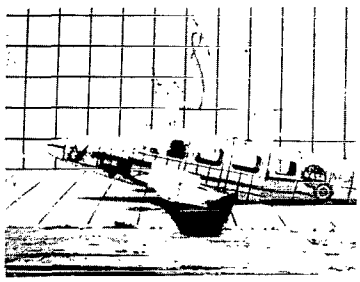

Time = 0.050 sec

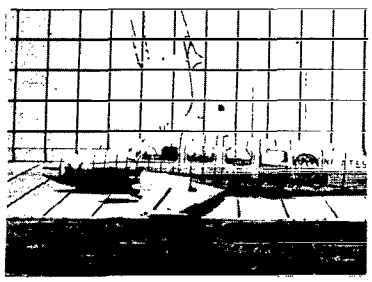

Time = 0.100 sec

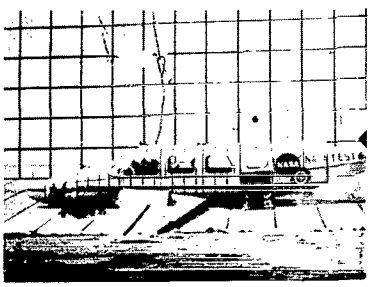

Time = 0.150 sec

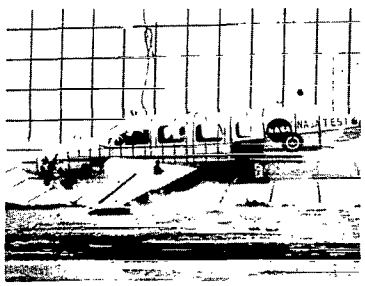

Time = 0.200 sec

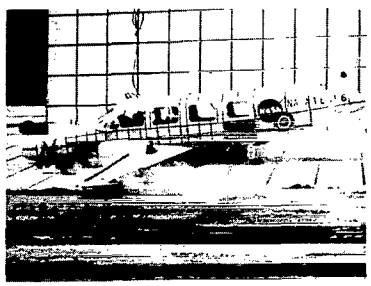

Time = 0.250 sec

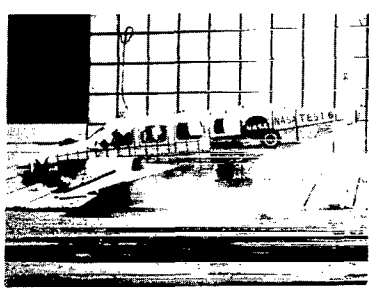

Time = 0.300 sec

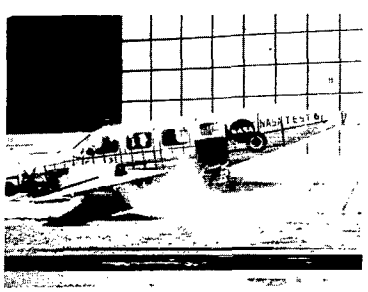

Time = 0.350 sec

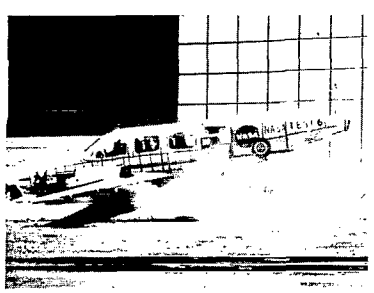

Time = 0.400 sec

(c) Pitch-up test.

L-79-304

Figure 11.- Concluded.

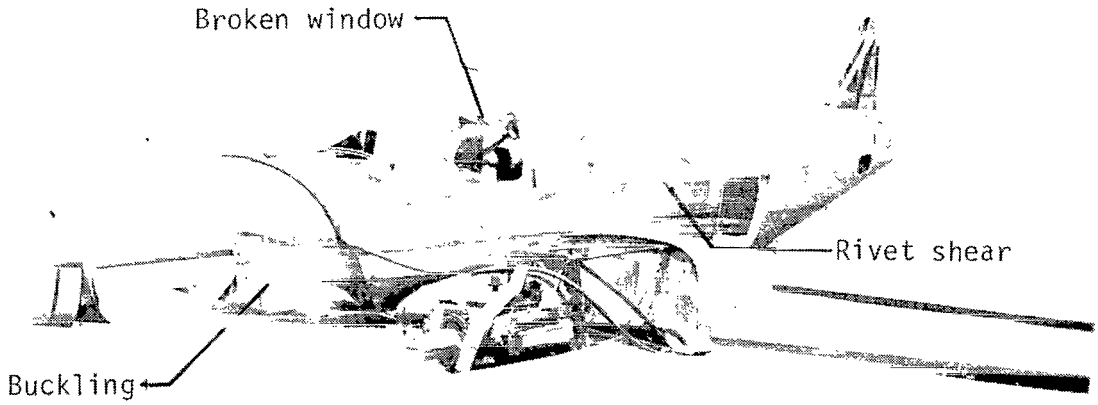

(a) Pitch-down test specimen.

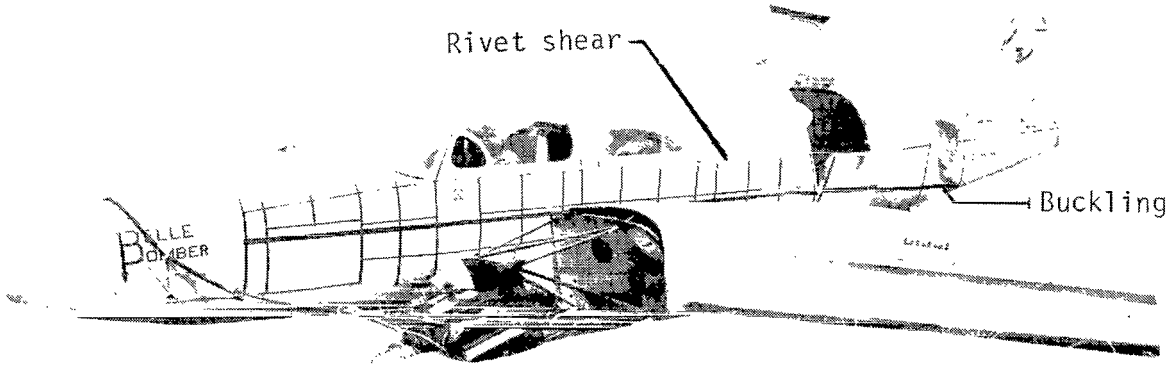

(b) Flat test specimen.

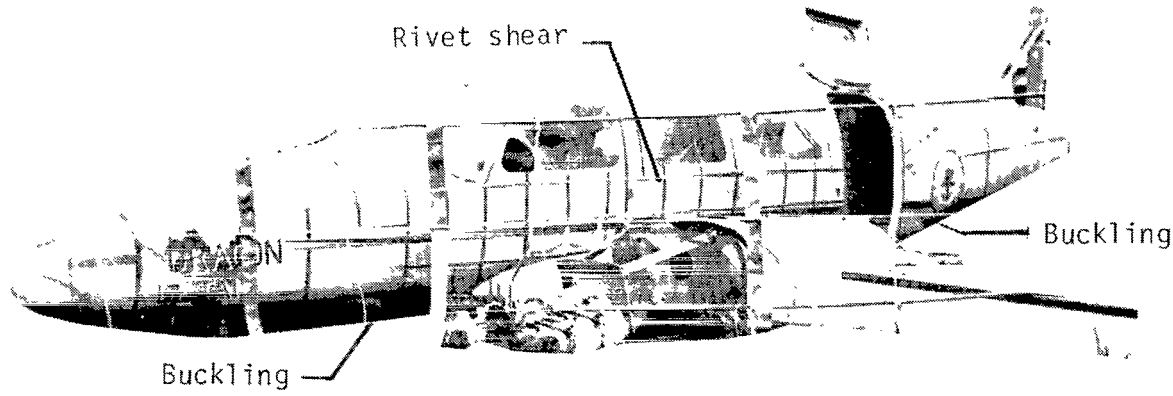

(c) Pitch-up test specimen.

L-79-305

Figure 12.- Postcrash comparison of airplane exterior damage of the three test specimens.

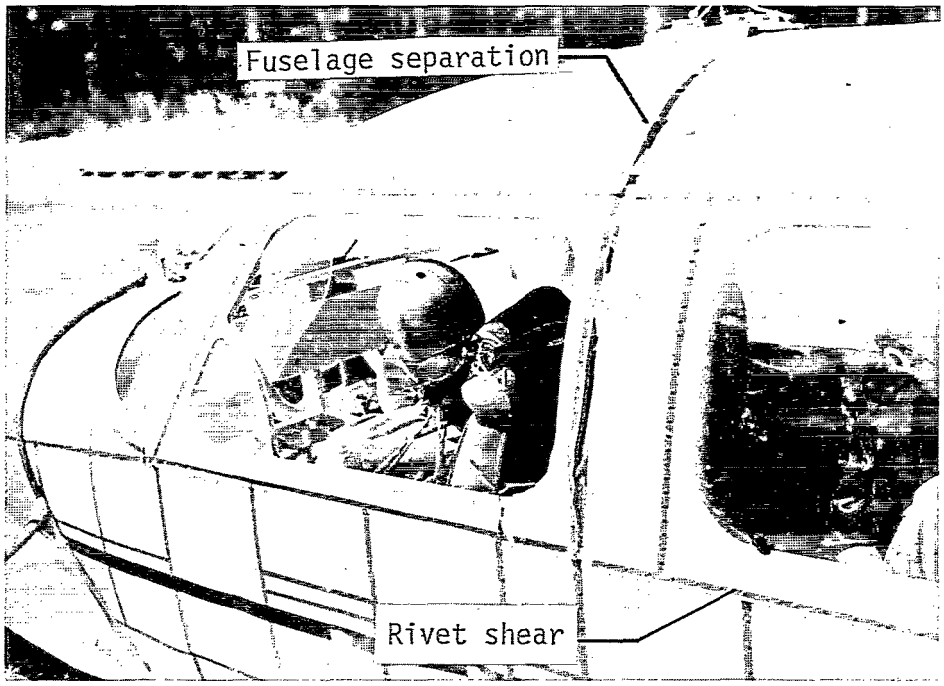

L-74-2632.1

(a) Separation of fuselage on port side of fuselage.

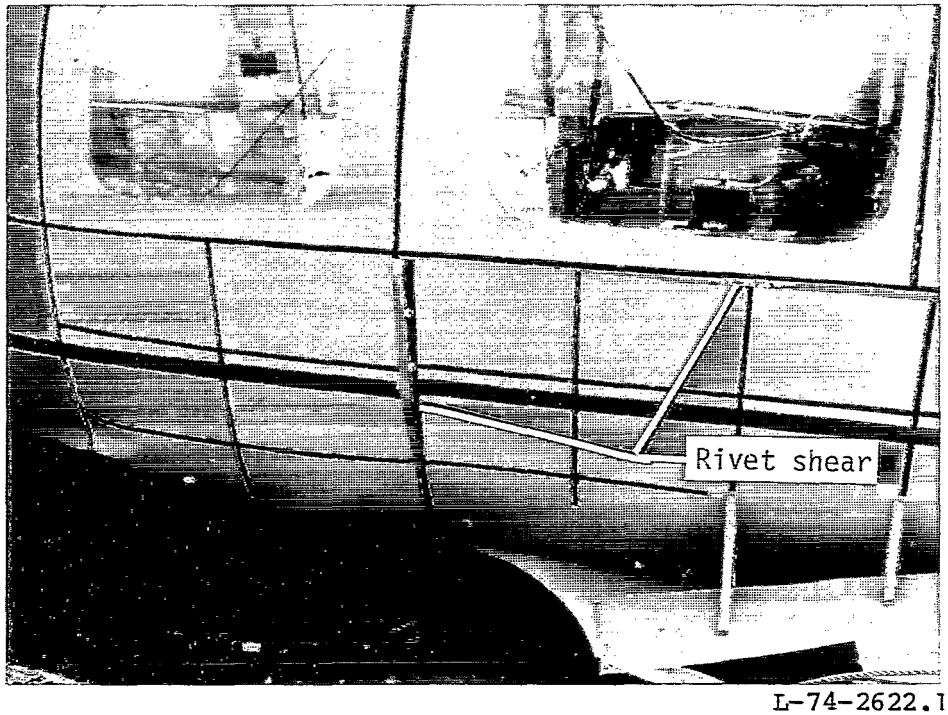

L-74-2622.1

(b) Separation of cabin on starboard side of fuselage.

Figure 13.- Postcrash exterior damage to pitch-down test specimen.

L-74-8081.1

(a) Aft section damage on starboard side of fuselage.

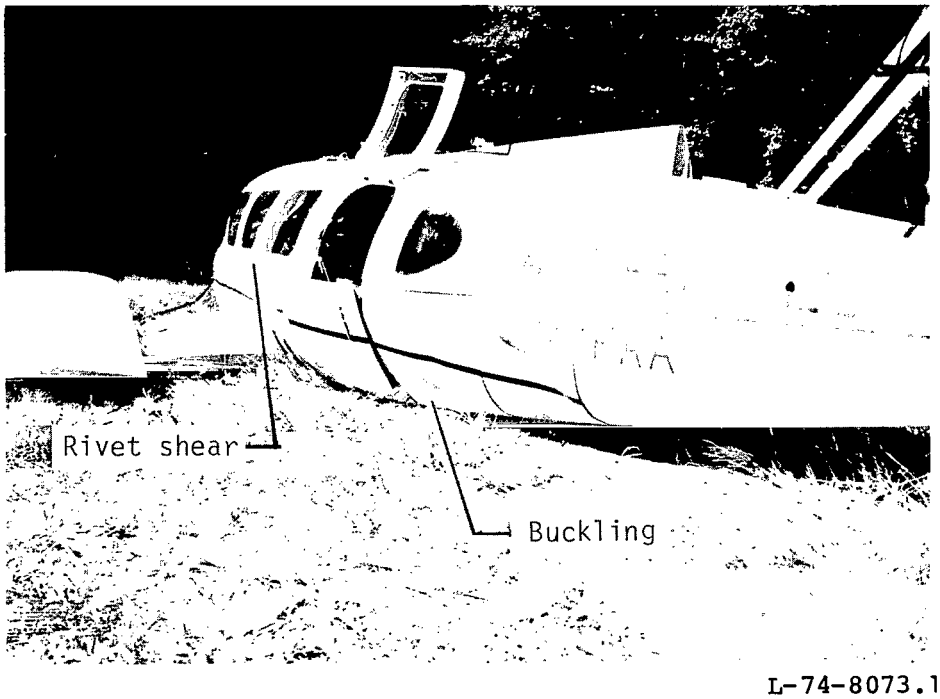

L-74-8073.1

(b) Aft section damage on port side of fuselage.

Figure 14.- Postcrash exterior damage to flat test specimen.

L-75-3755.1

(a) Aft section damage on port side of fuselage.

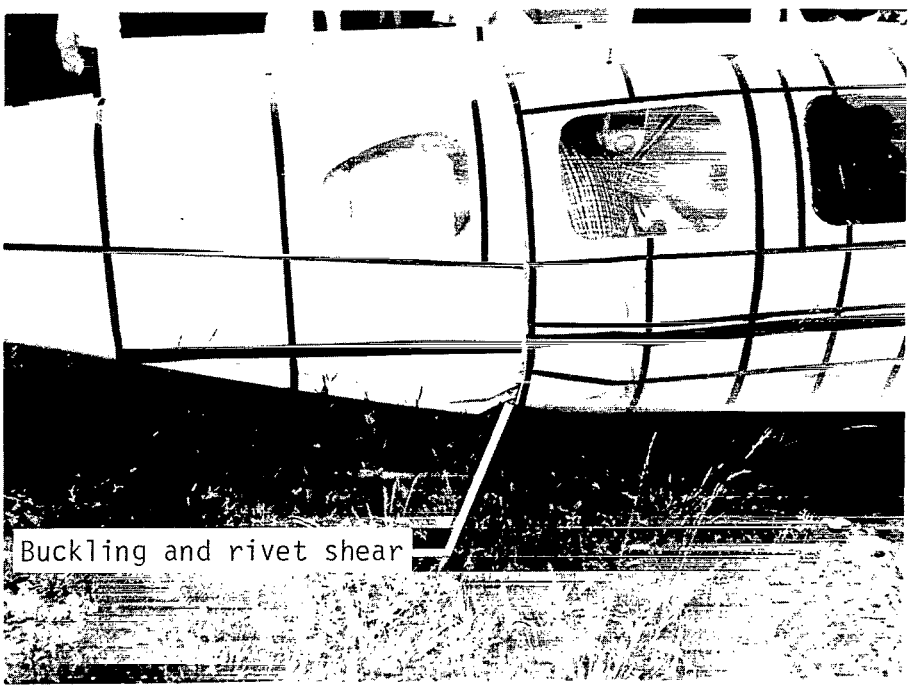

L-75-3749.1

(b) Aft section damage on starboard side of fuselage.

Figure 15.- Postcrash exterior damage to pitch-up test specimen.

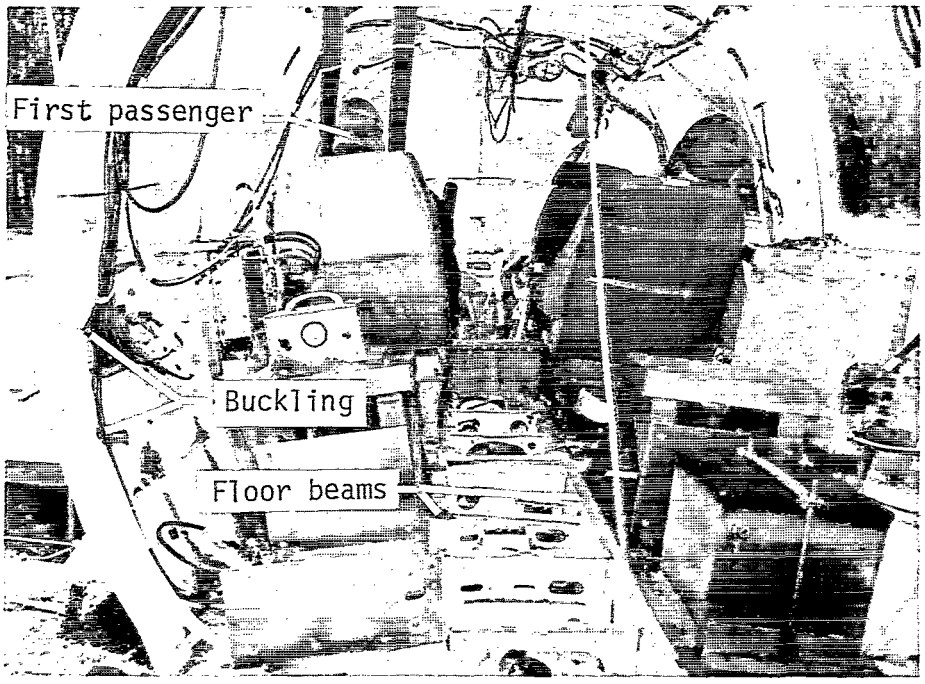

L-74-2642.1

(a) View looking forward.

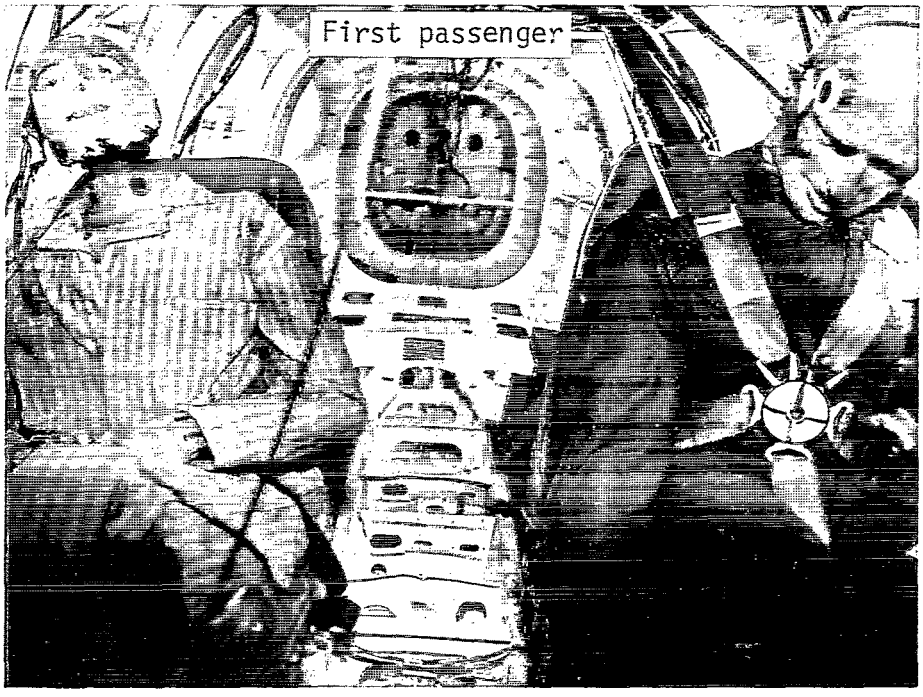

L-74-2638.1

(b) View looking aft.

Figure 16.- Postcrash interior damage to pitch-down test specimen.

L-74-8078.1

(a) View looking forward.

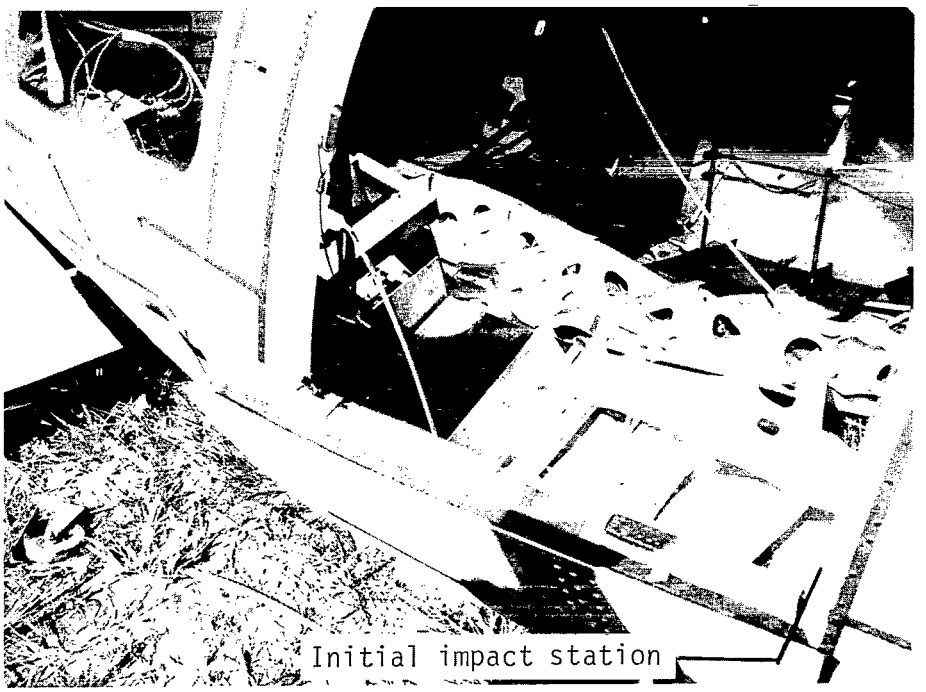

L-74-8079.1

(b) View looking at floor through fuselage door.

Figure 17.- Postcrash interior damage to flat test specimen.

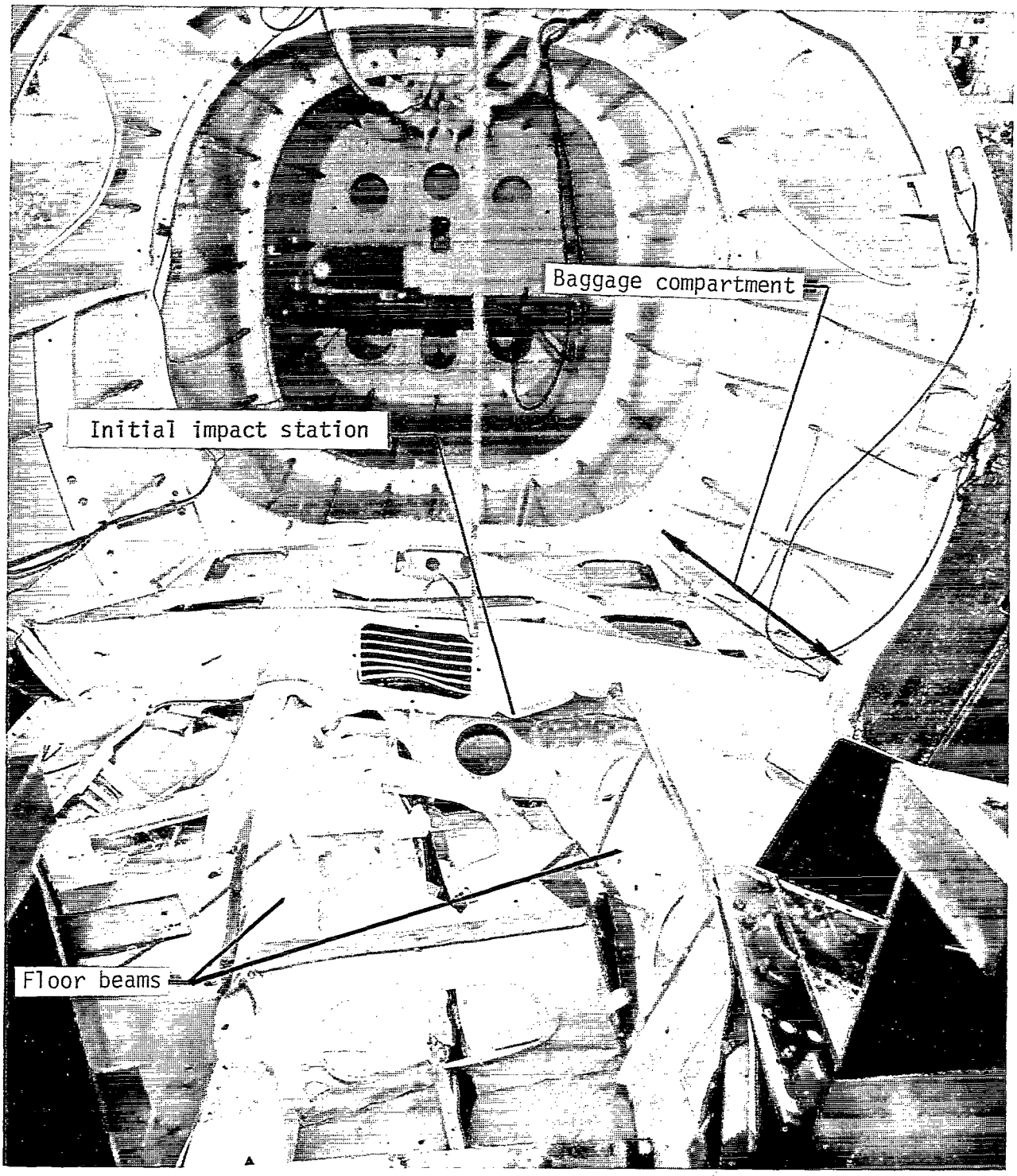

L-79-306

(c) View looking aft.

Figure 17.- Continued.

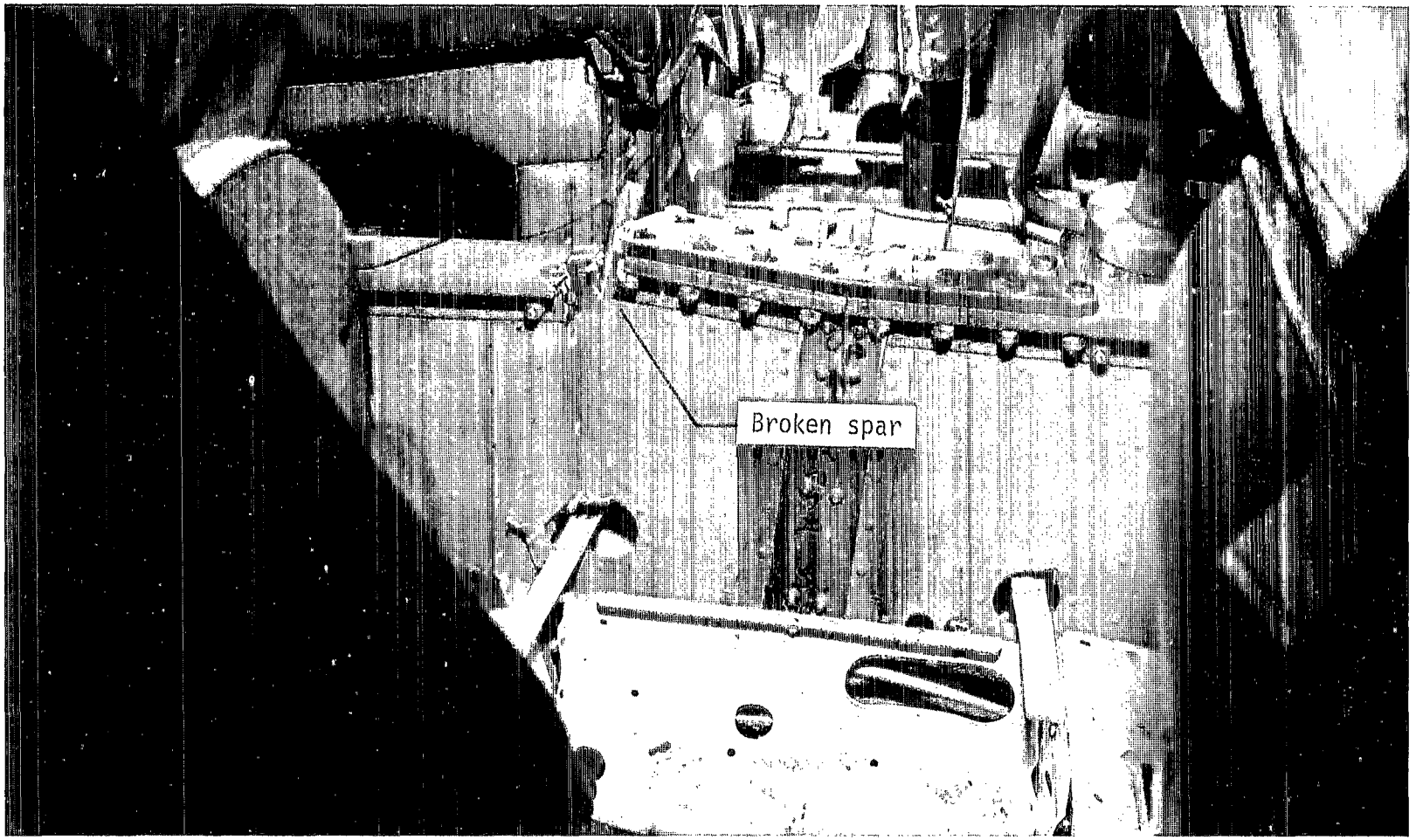

L-74-8075.1

(d) View of broken main wing spar.

Figure 17.- Concluded.

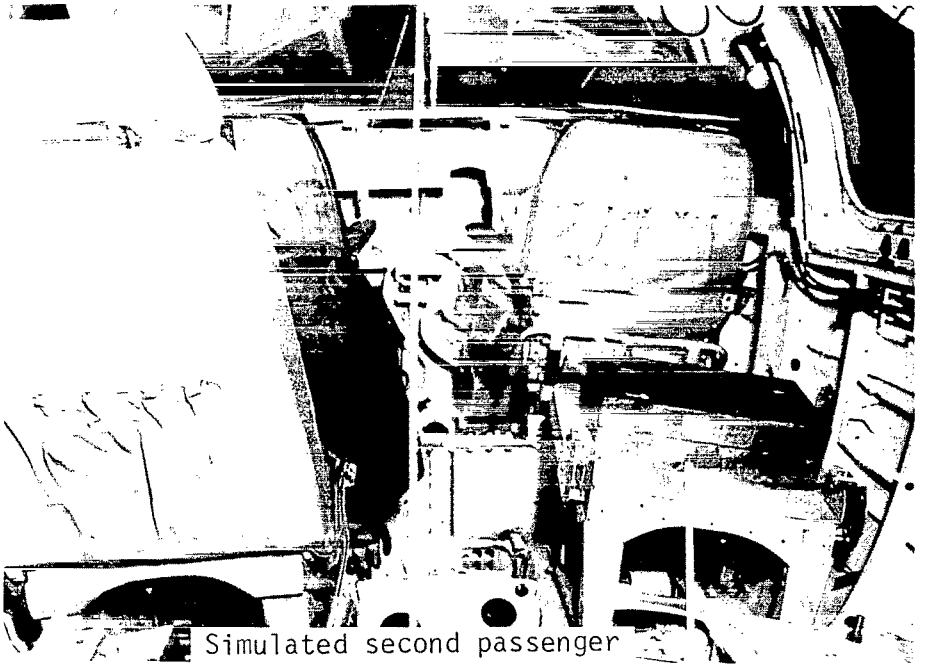

L-75-3760.1

(a) View looking forward.

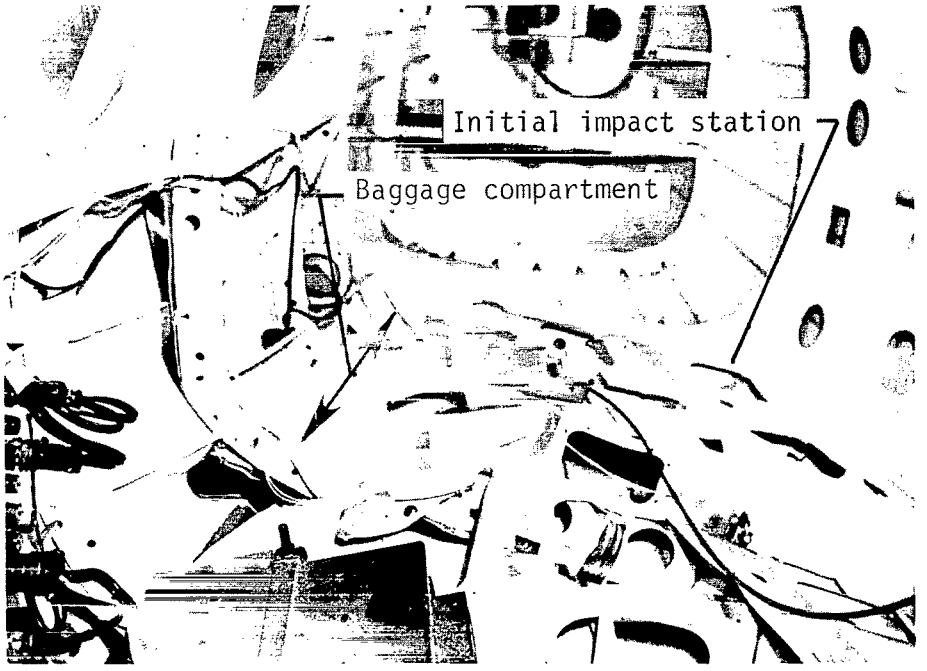

L-75-3759.1

(b) View looking aft.

Figure 18.- Postcrash interior damage to pitch-up test specimen.

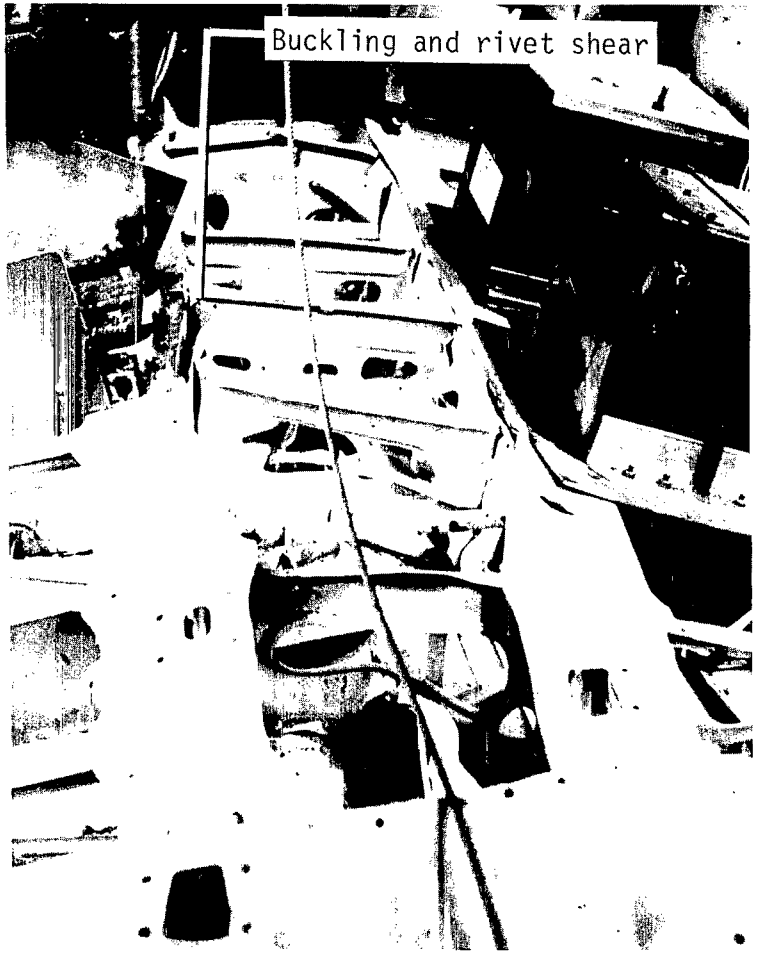

L-79-307

(c) View of floor in aft section of cabin.

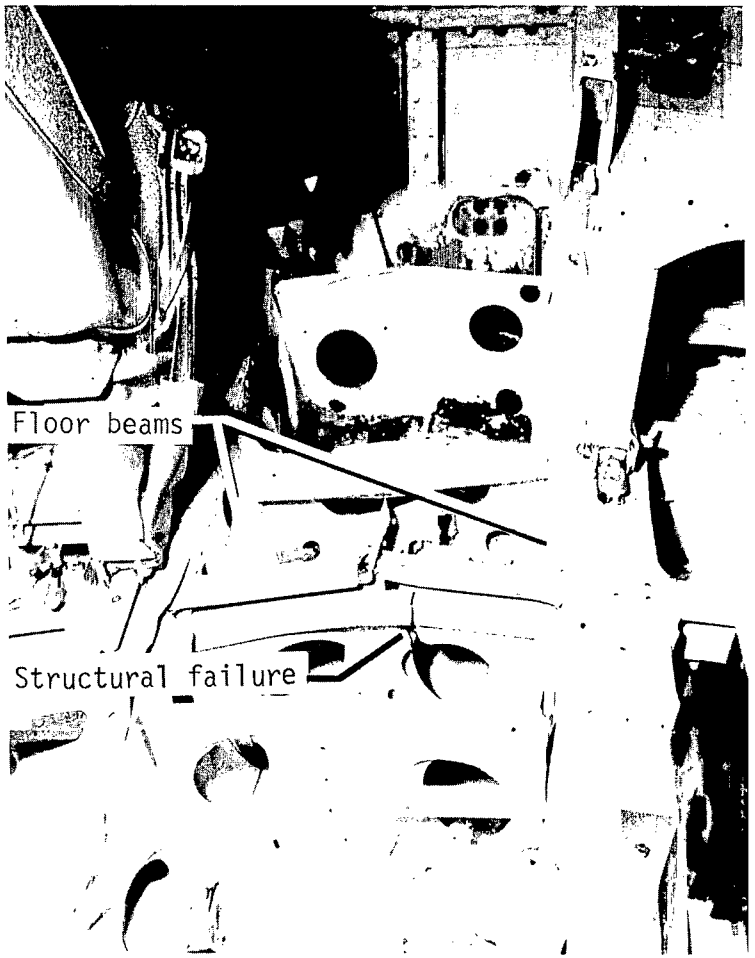

L-75-3748.1

(d) View of floor between first- and second-passenger seats.

Figure 18.- Concluded.

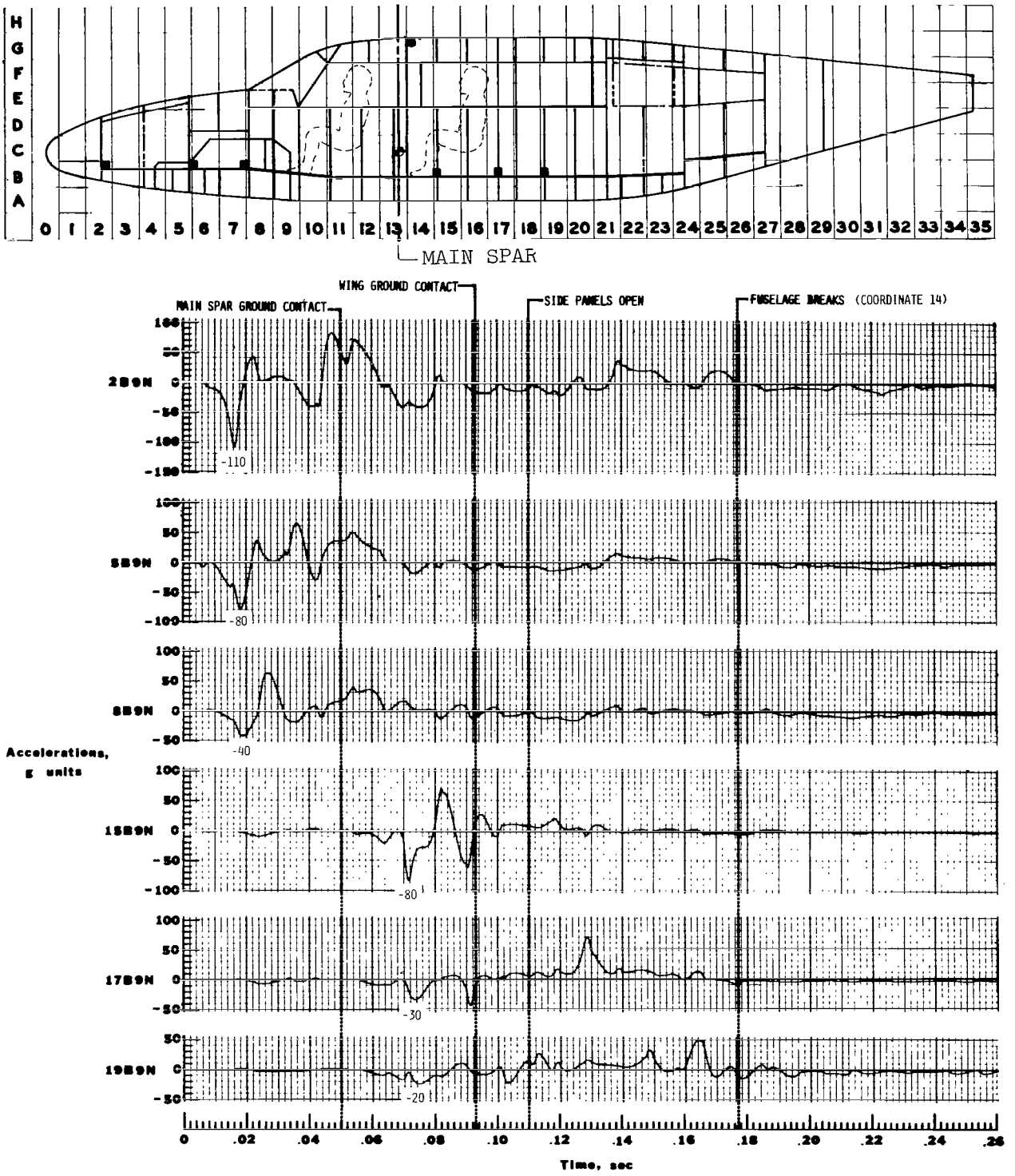

(a) Pitch-down test.

Figure 19.- Histories of the floor-beam normal accelerations.

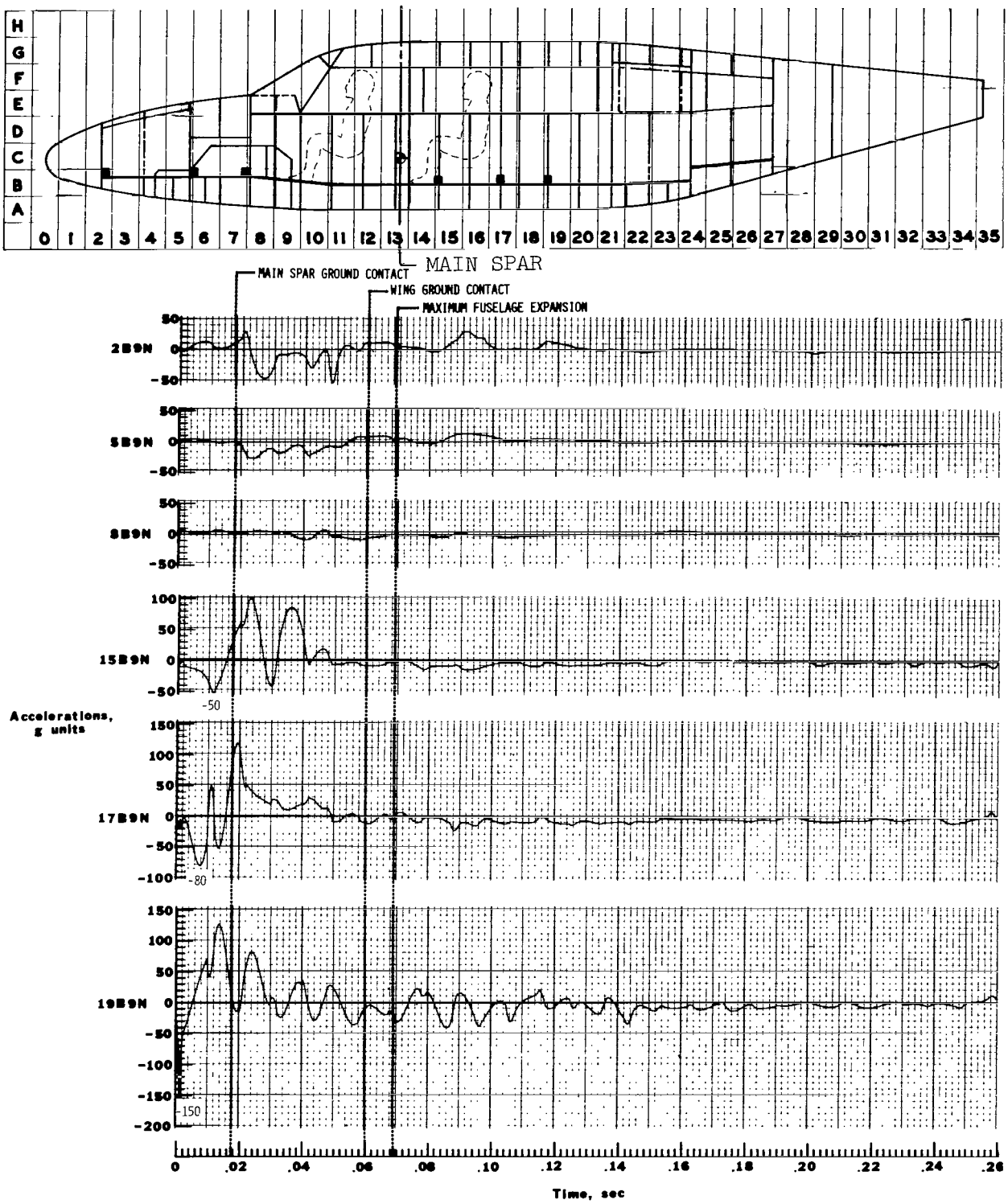

(b) Flat test.

Figure 19.- Continued.

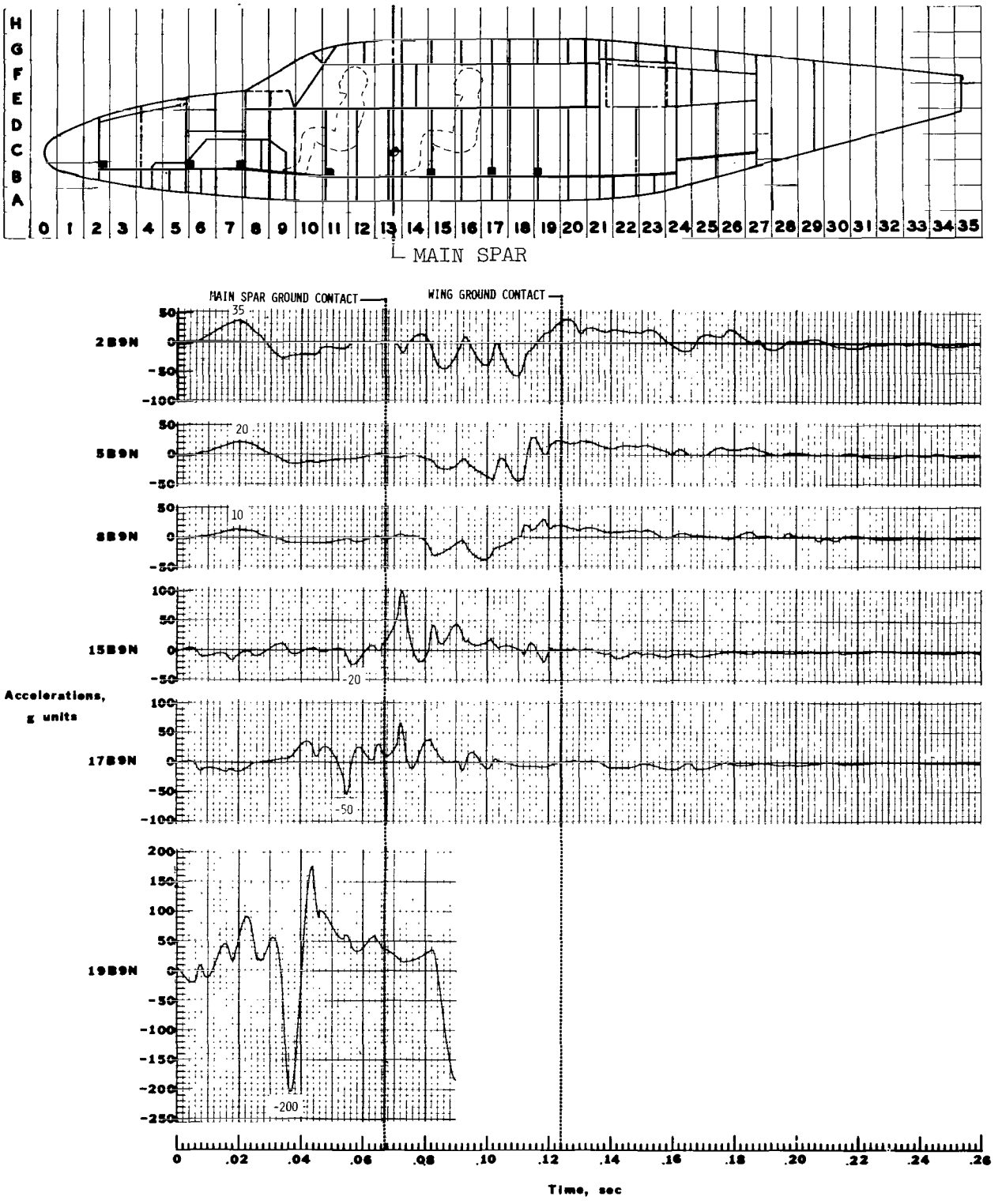

(c) Pitch-up test.

Figure 19.- Concluded.

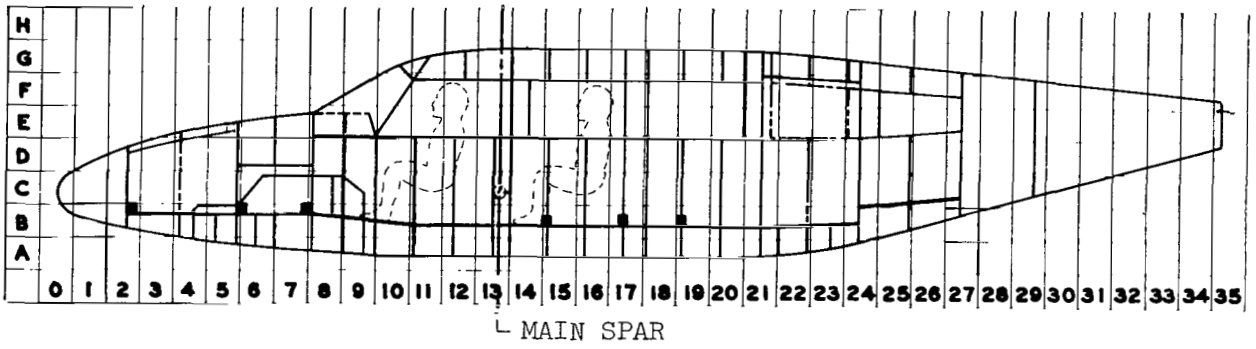

(a) Pitch-down test.

Figure 20.- Histories of the floor-beam longitudinal accelerations.

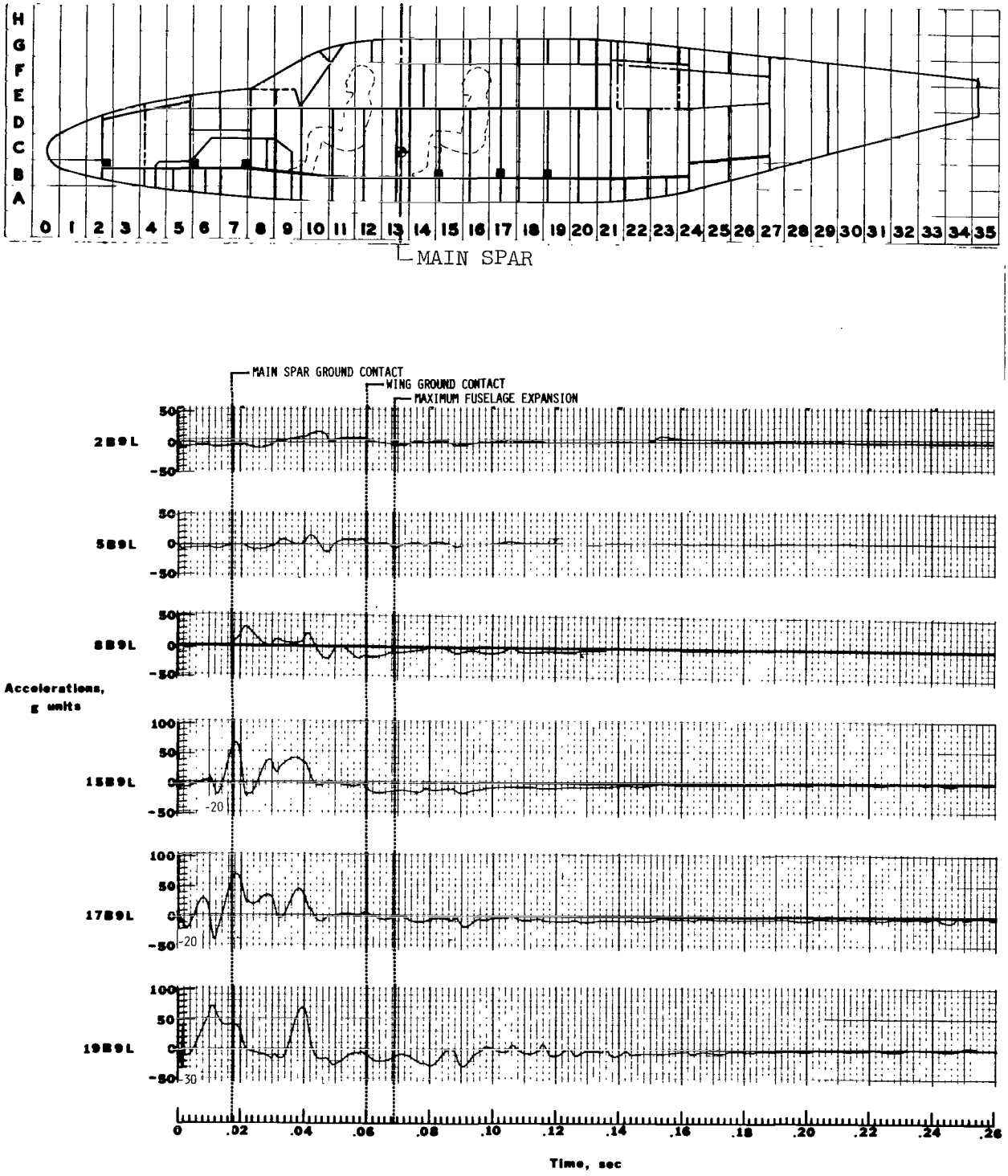

(b) Flat test.

Figure 20.- Continued.

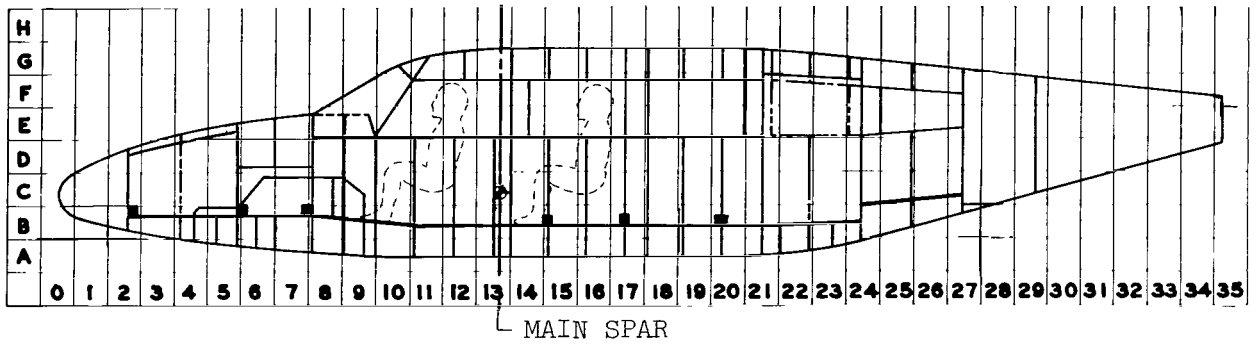

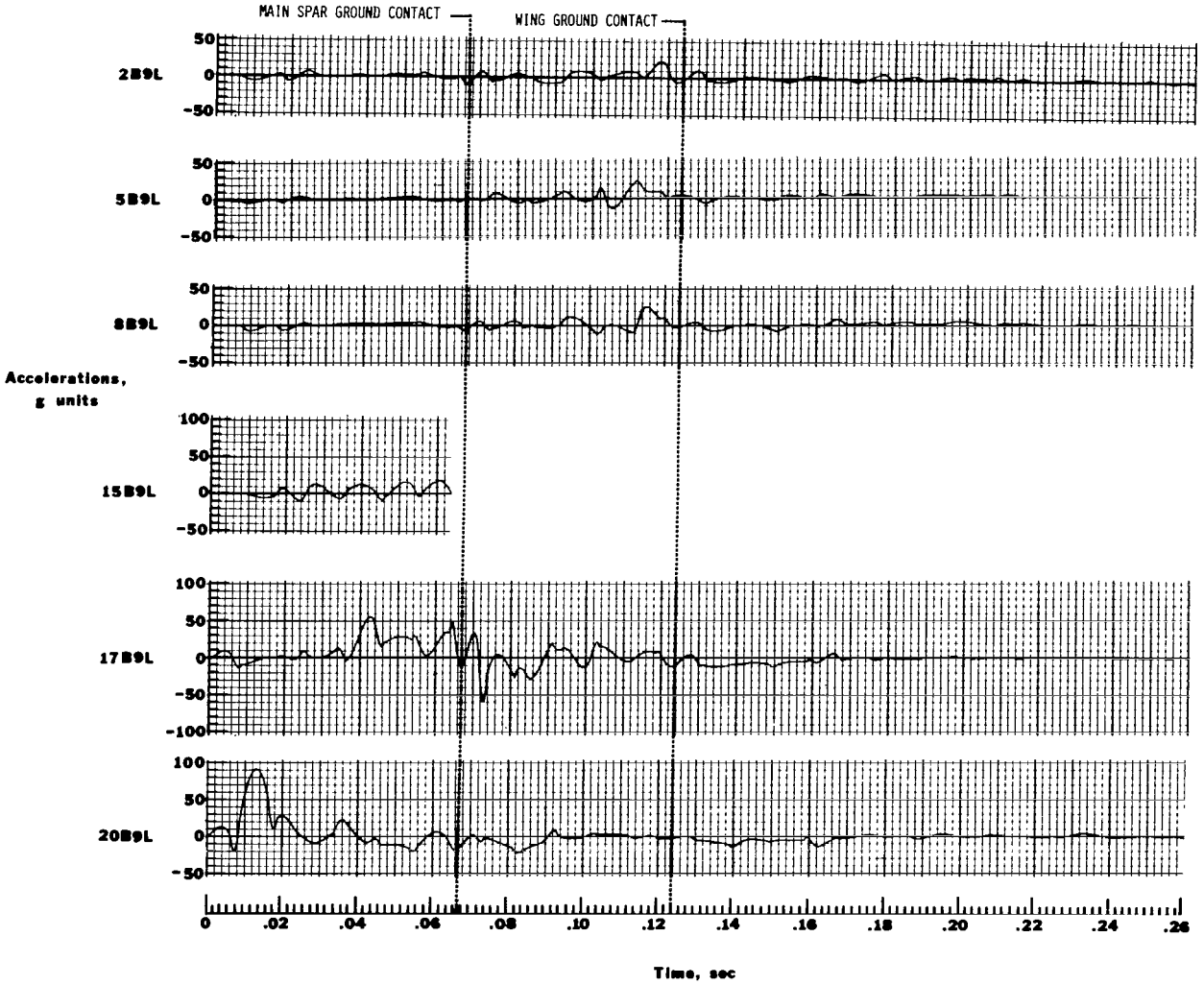

(c) Pitch-up test.

Figure 20.- Concluded.

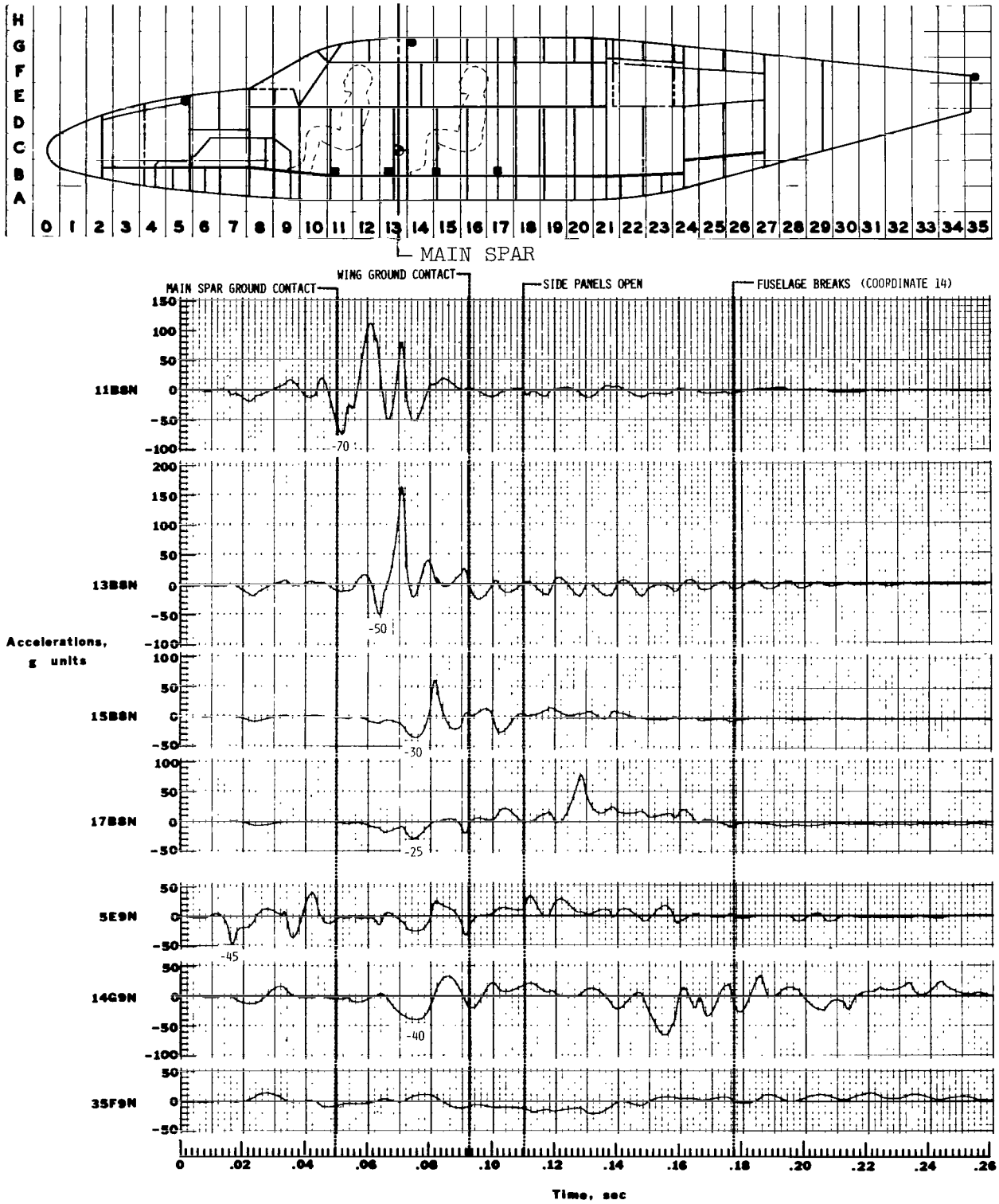

(a) Pitch-down test.

Figure 21.- Histories of roof and floor normal accelerations.

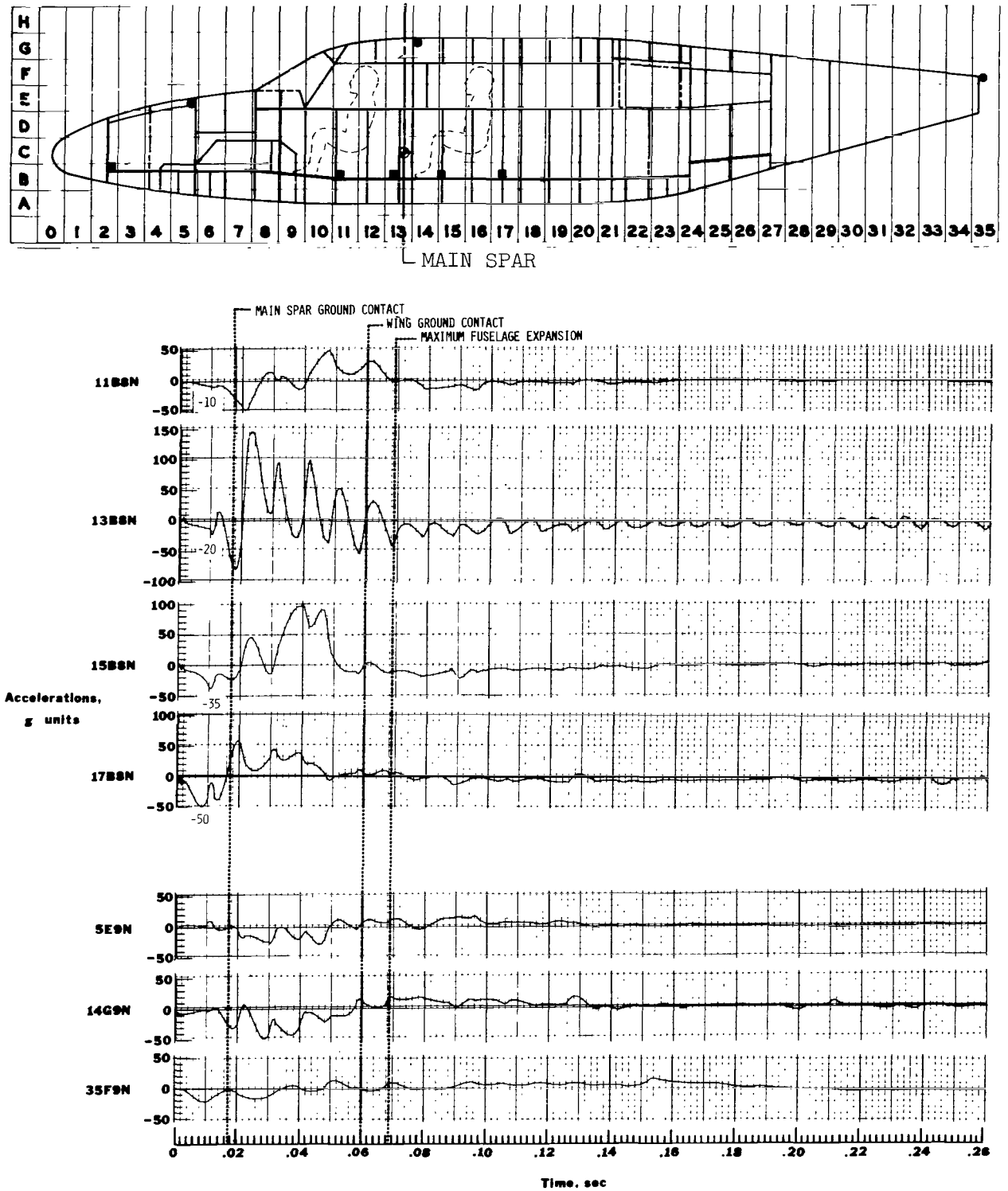

(b) Flat test.

Figure 21.- Continued.

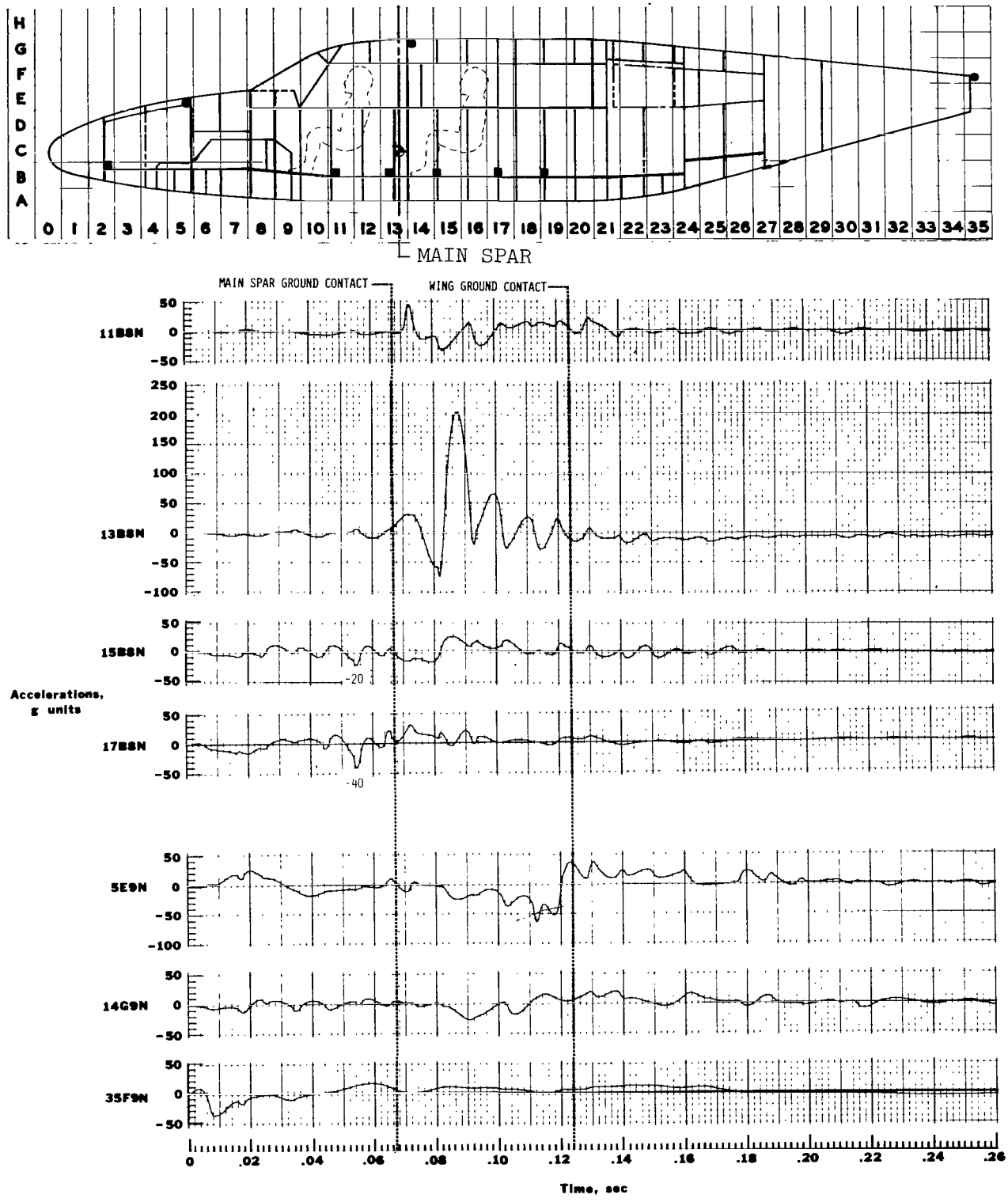

(c) Pitch-up test.

Figure 21.- Concluded.

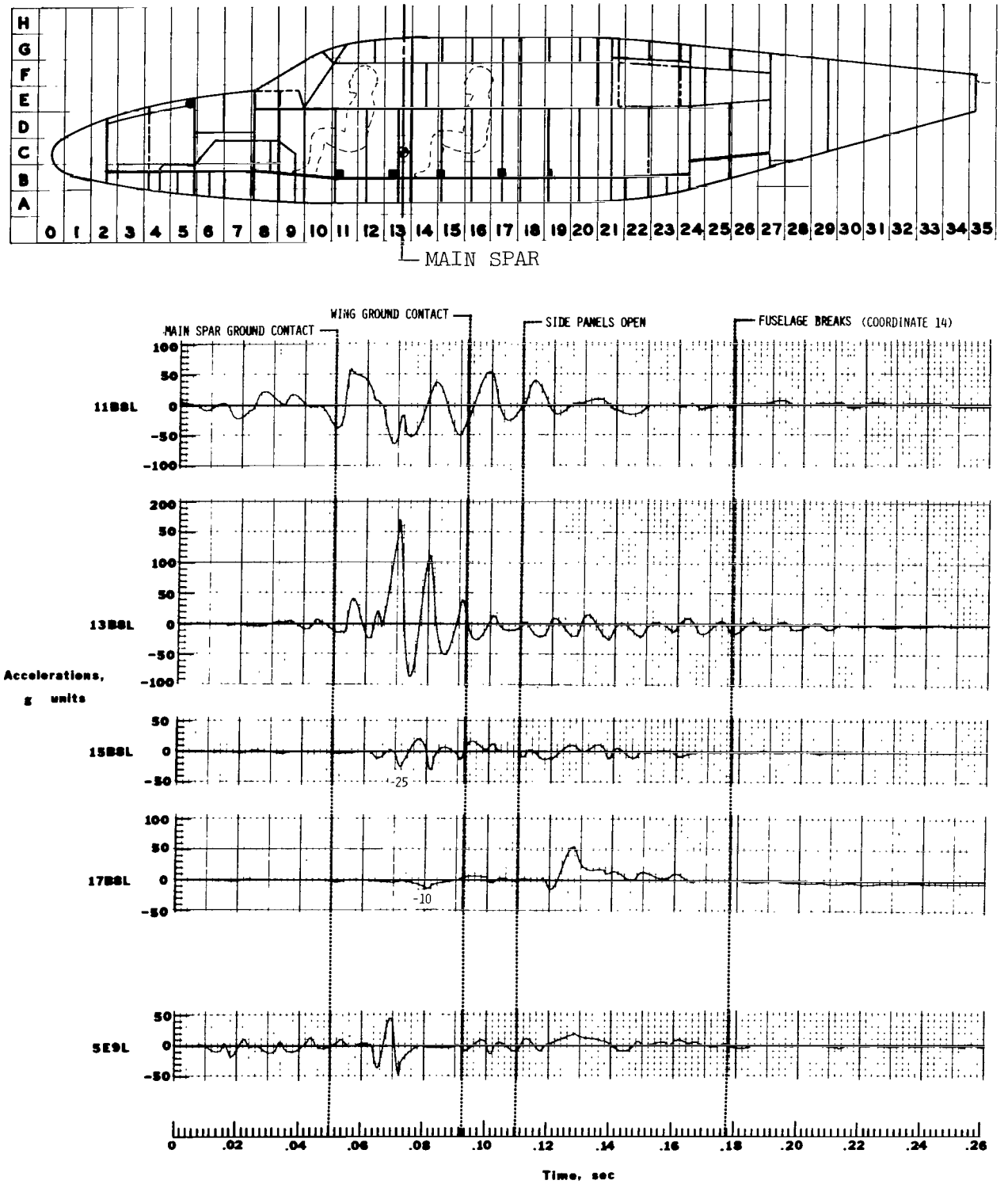

(a) Pitch-down test.

Figure 22.- Histories of roof and floor longitudinal accelerations.

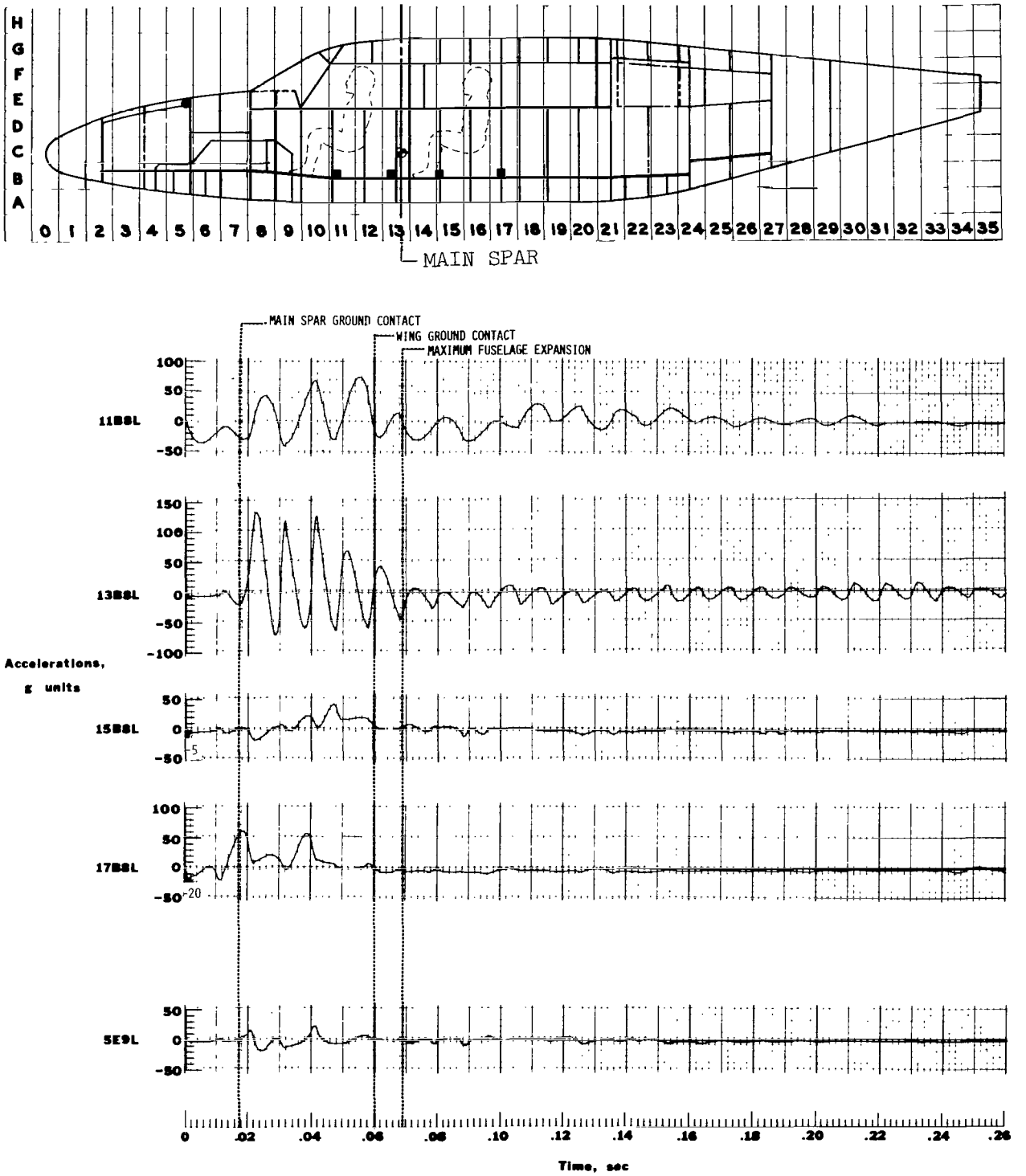

(b) Flat test.

Figure 22.- Continued.

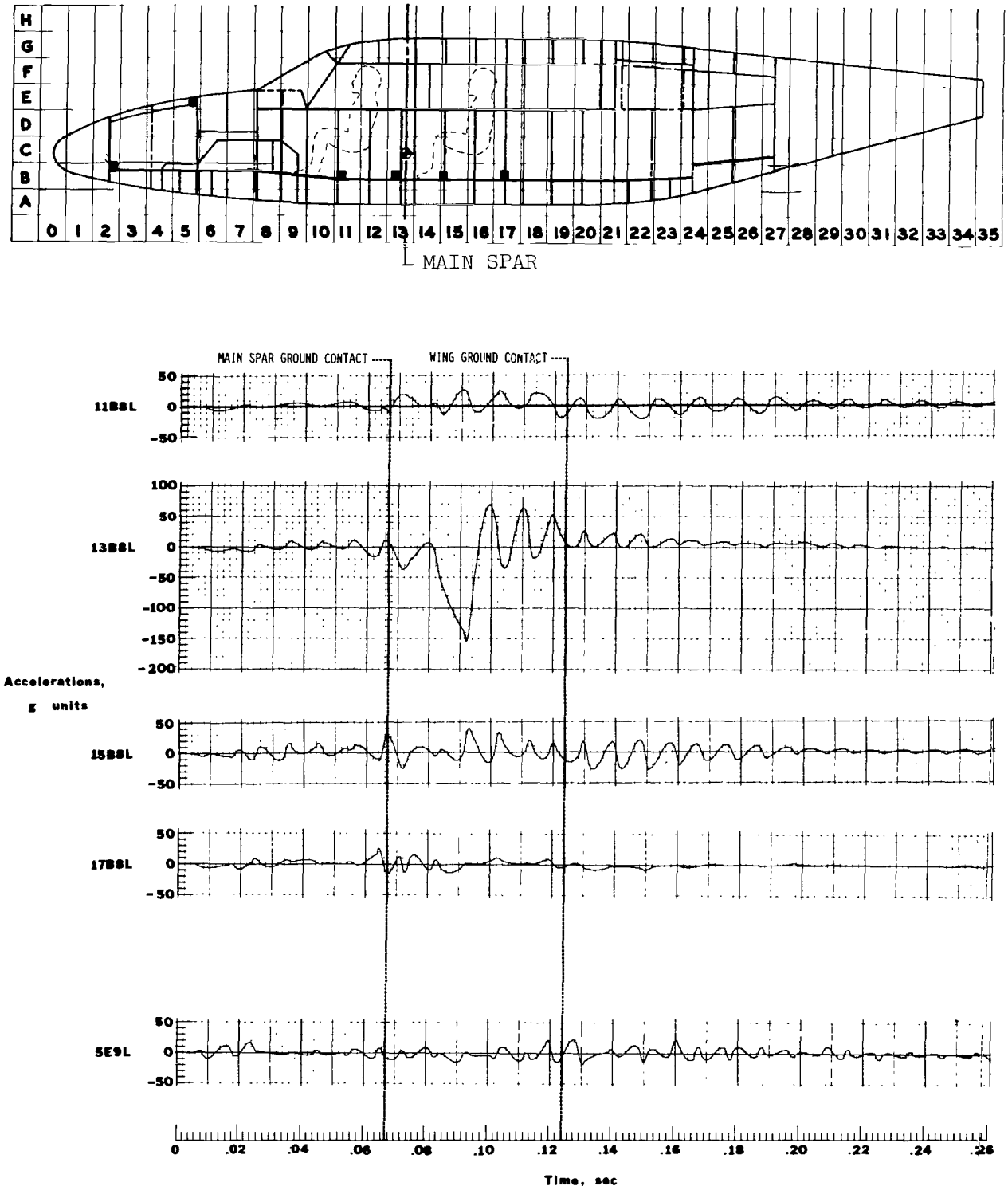

(c) Pitch-up test.

Figure 22.- Concluded.

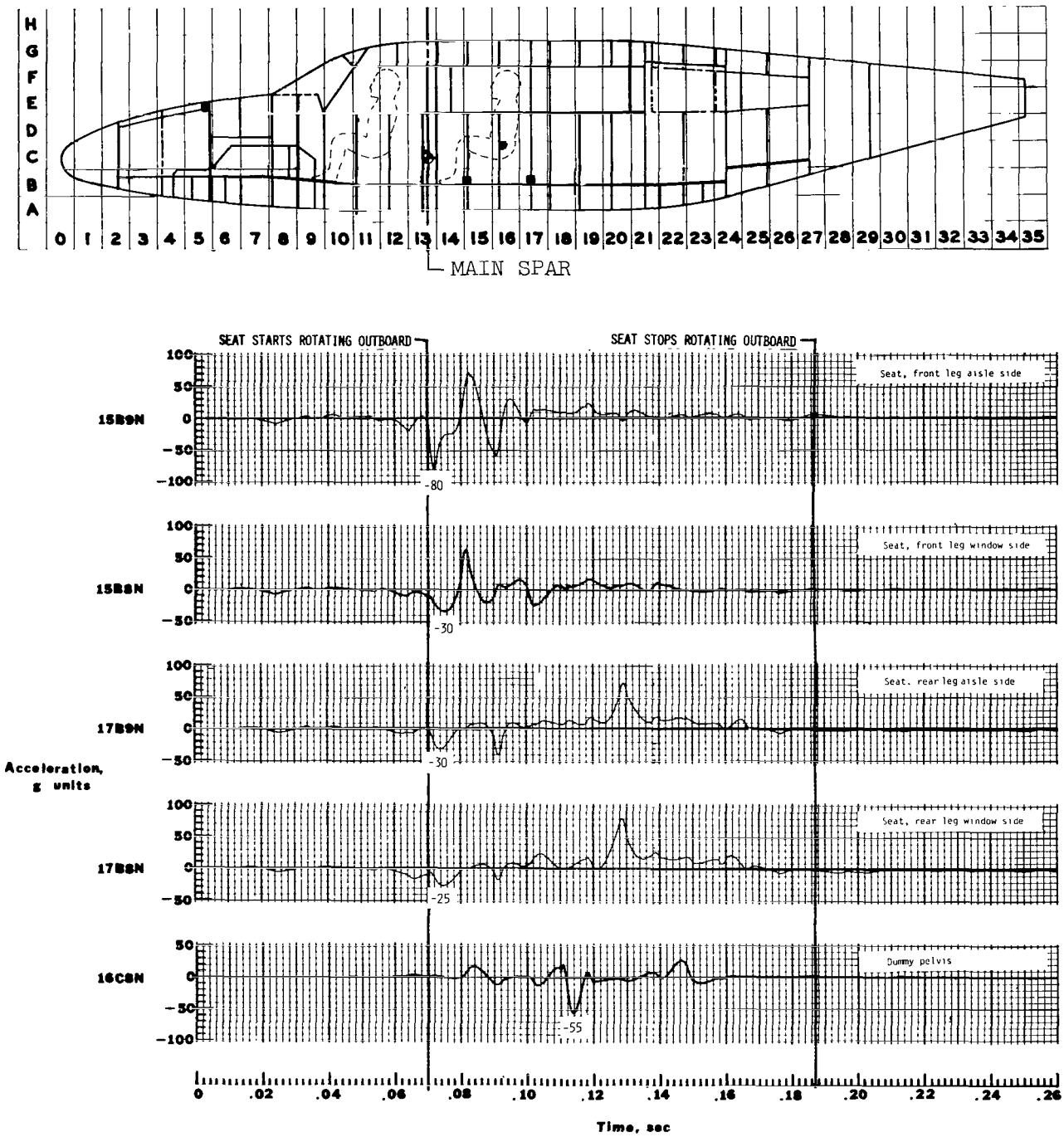

(a) Normal accelerations in pitch-down test.

Figure 23.- Histories of normal accelerations on floor at first-passenger seat legs and in dummy.

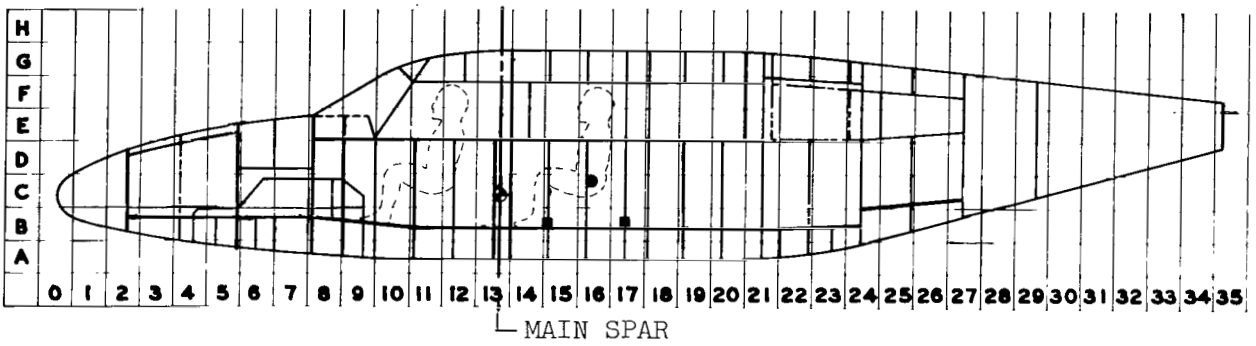

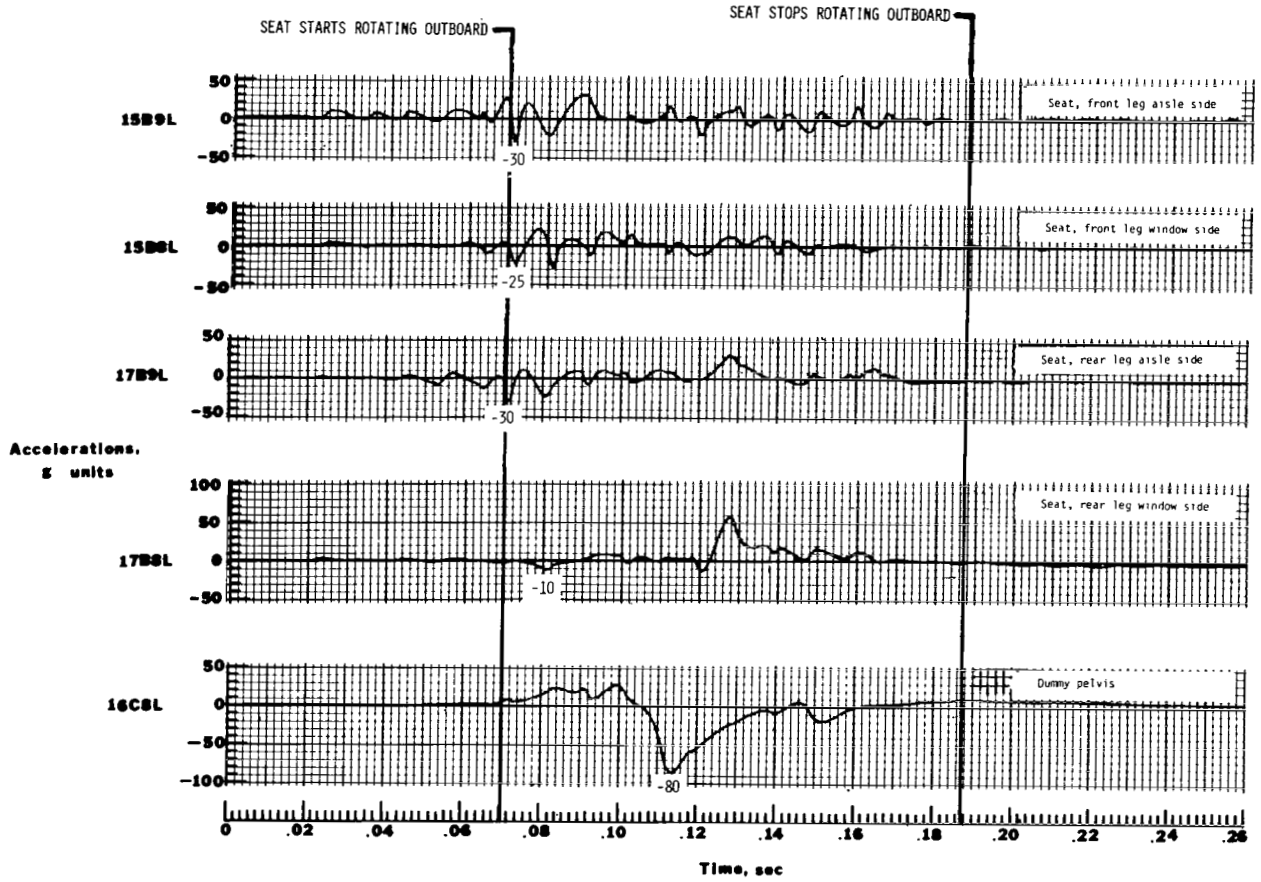

(b) Longitudinal accelerations in pitch-down test.

Figure 23.- Continued.

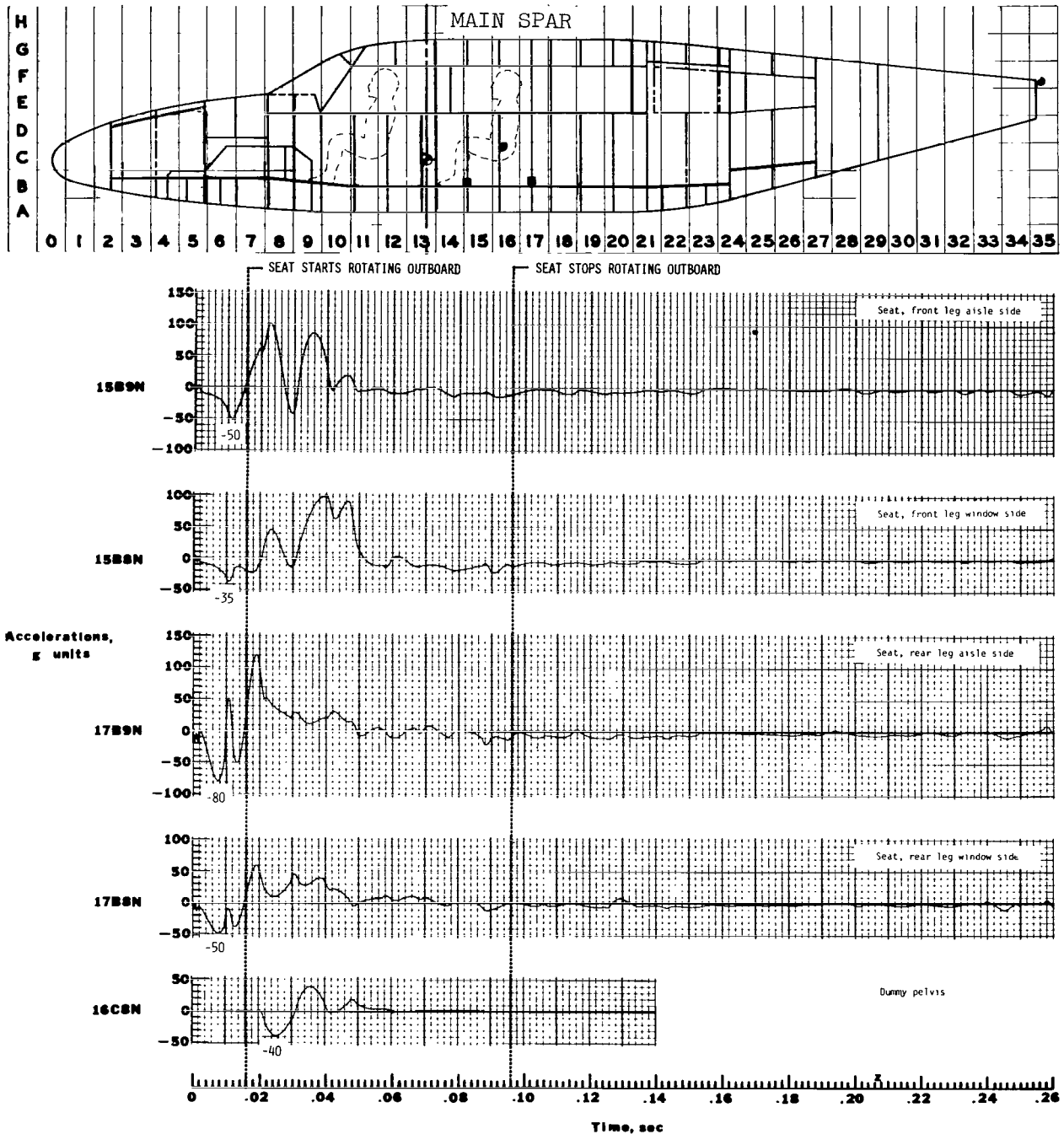

(c) Normal accelerations in flat test.

Figure 23.- Continued.

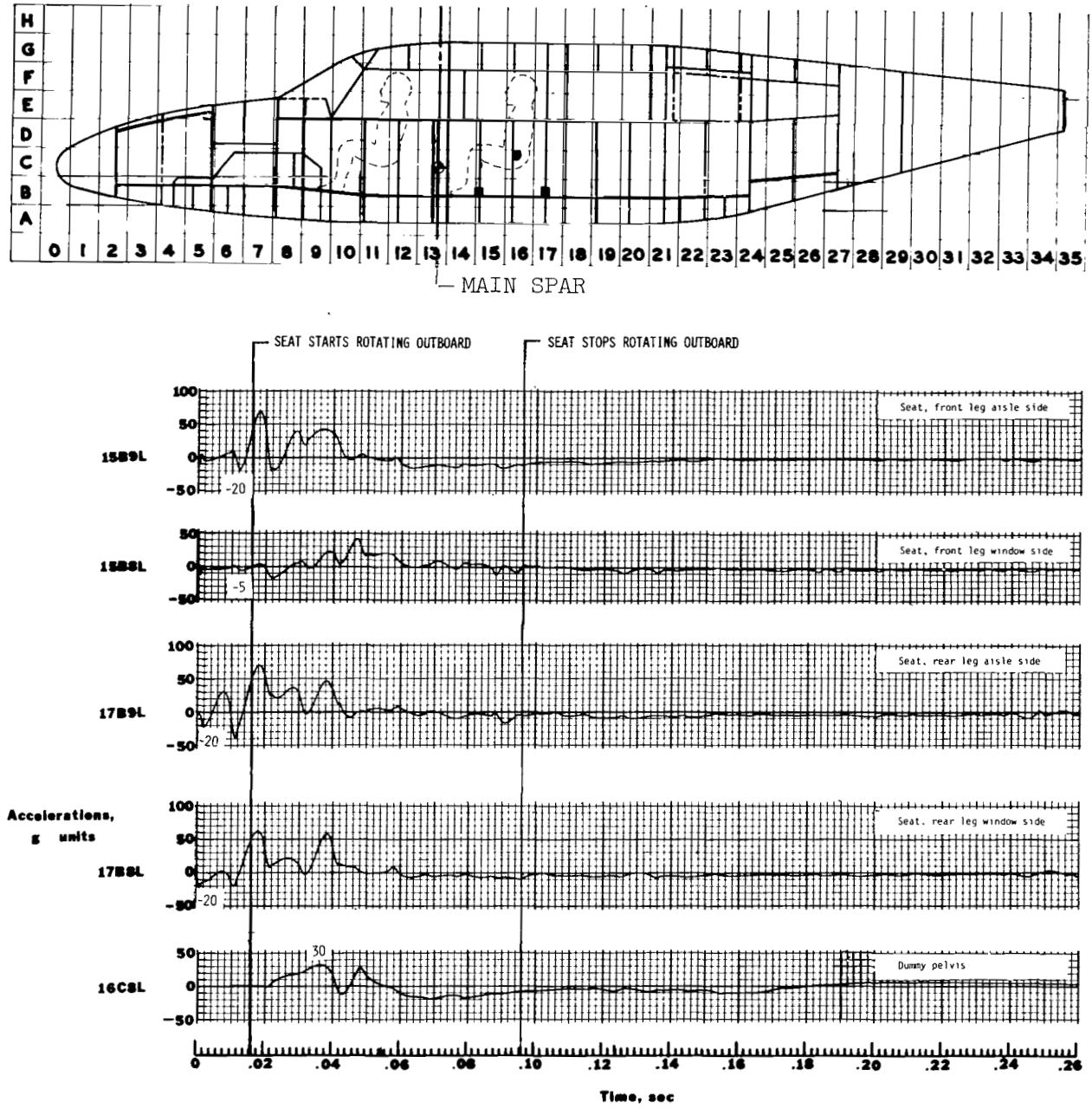

(d) Longitudinal accelerations in flat test.

Figure 23.- Continued.

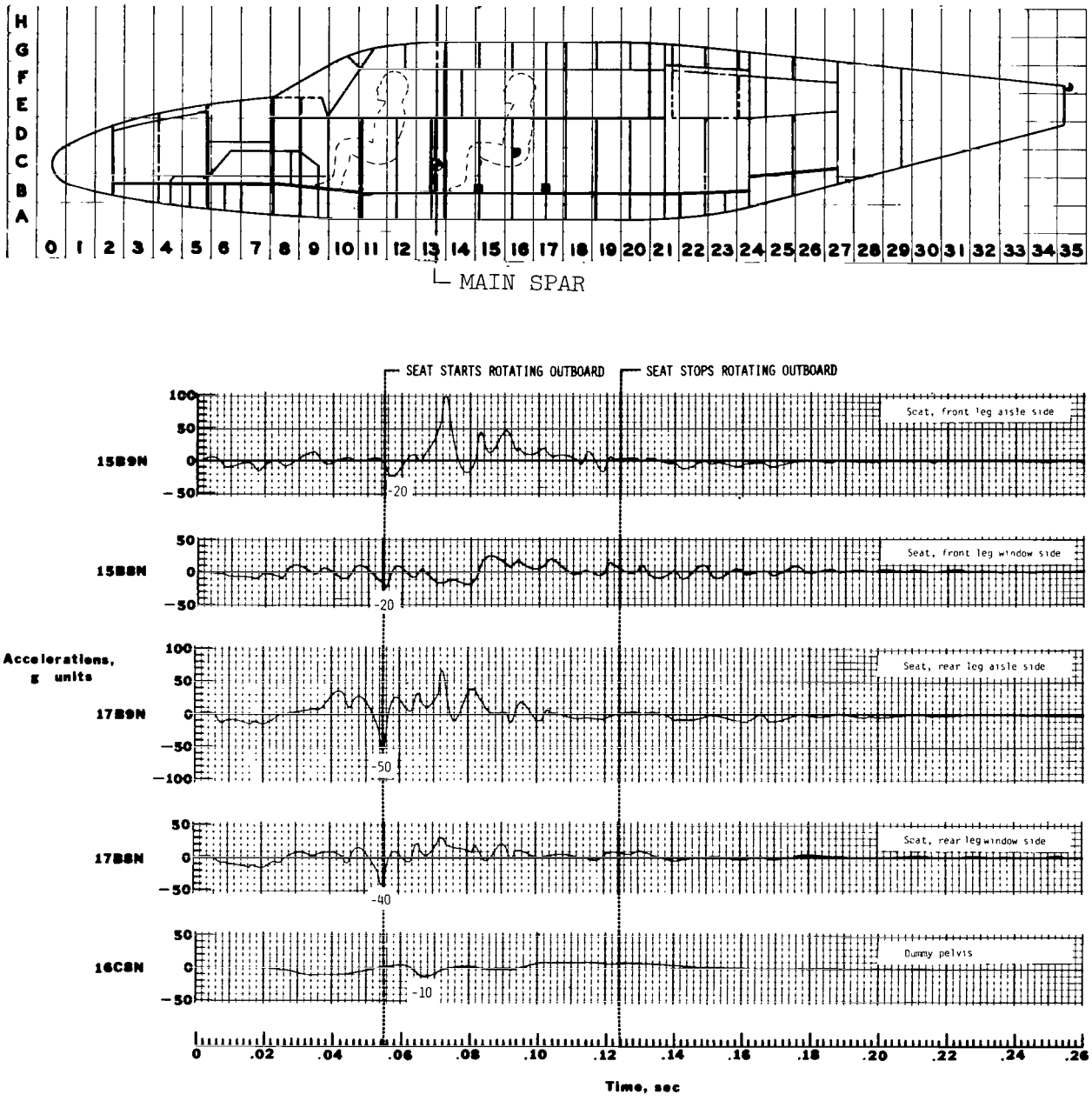

(e) Normal accelerations in pitch-up test.

Figure 23.- Continued.

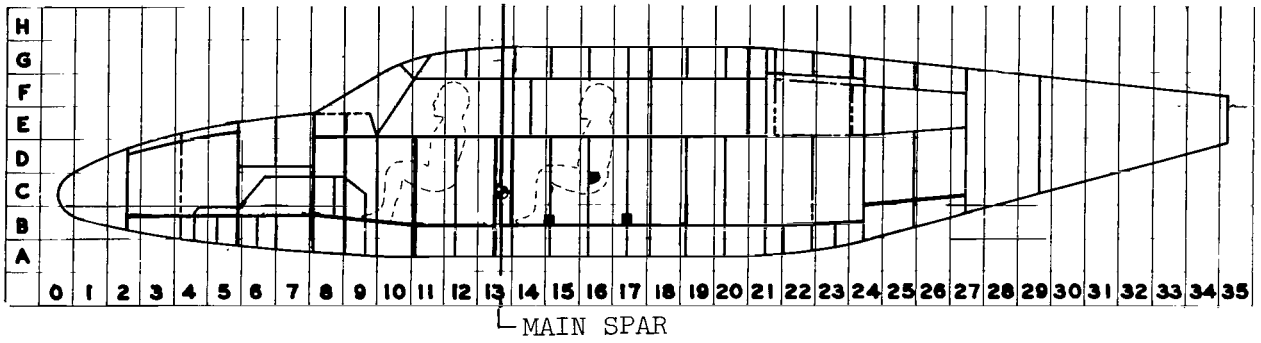

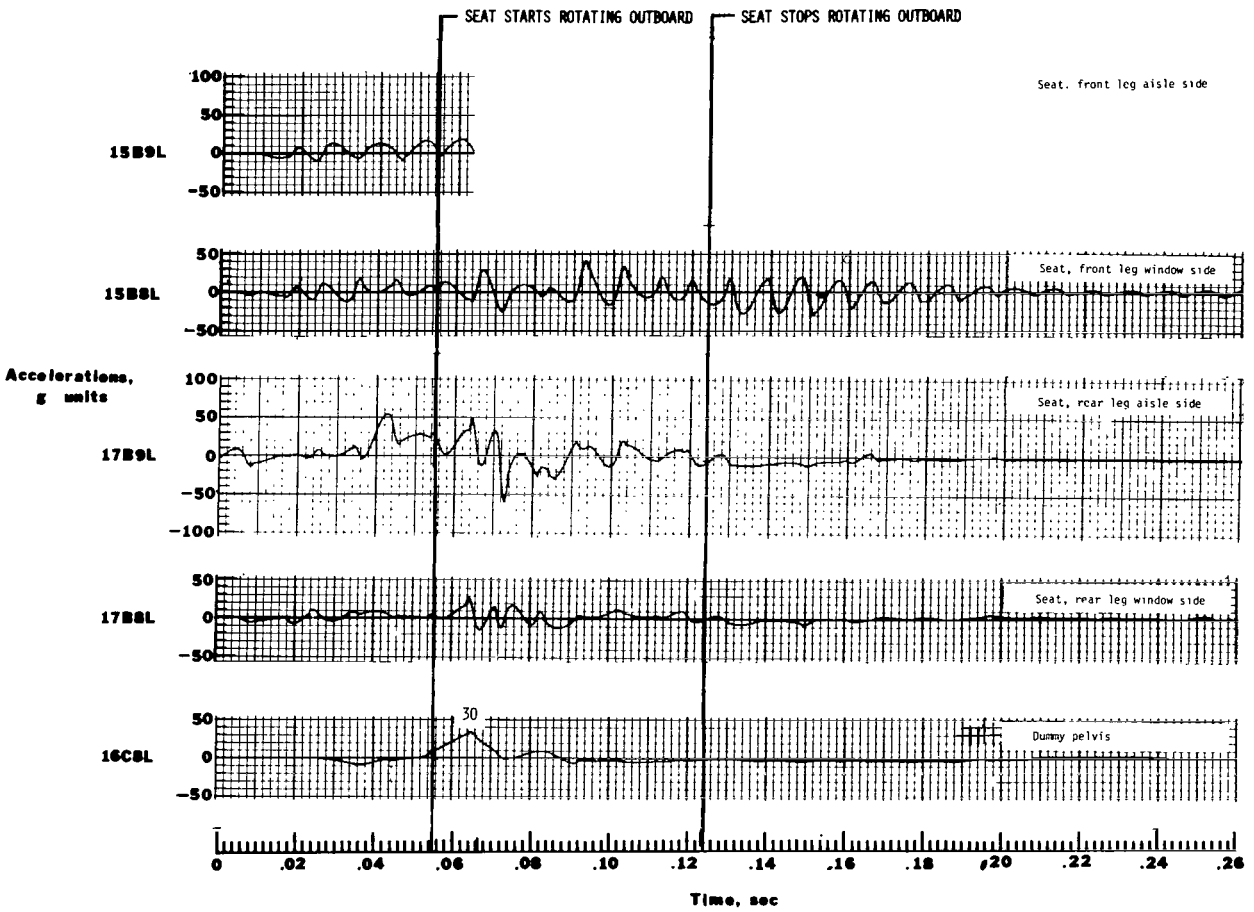

(f) Longitudinal accelerations in pitch-up test.

Figure 23.- Concluded.

L-75-3751

Figure 24.- Submarined position of first-passenger dummy in pitch-up test specimen.

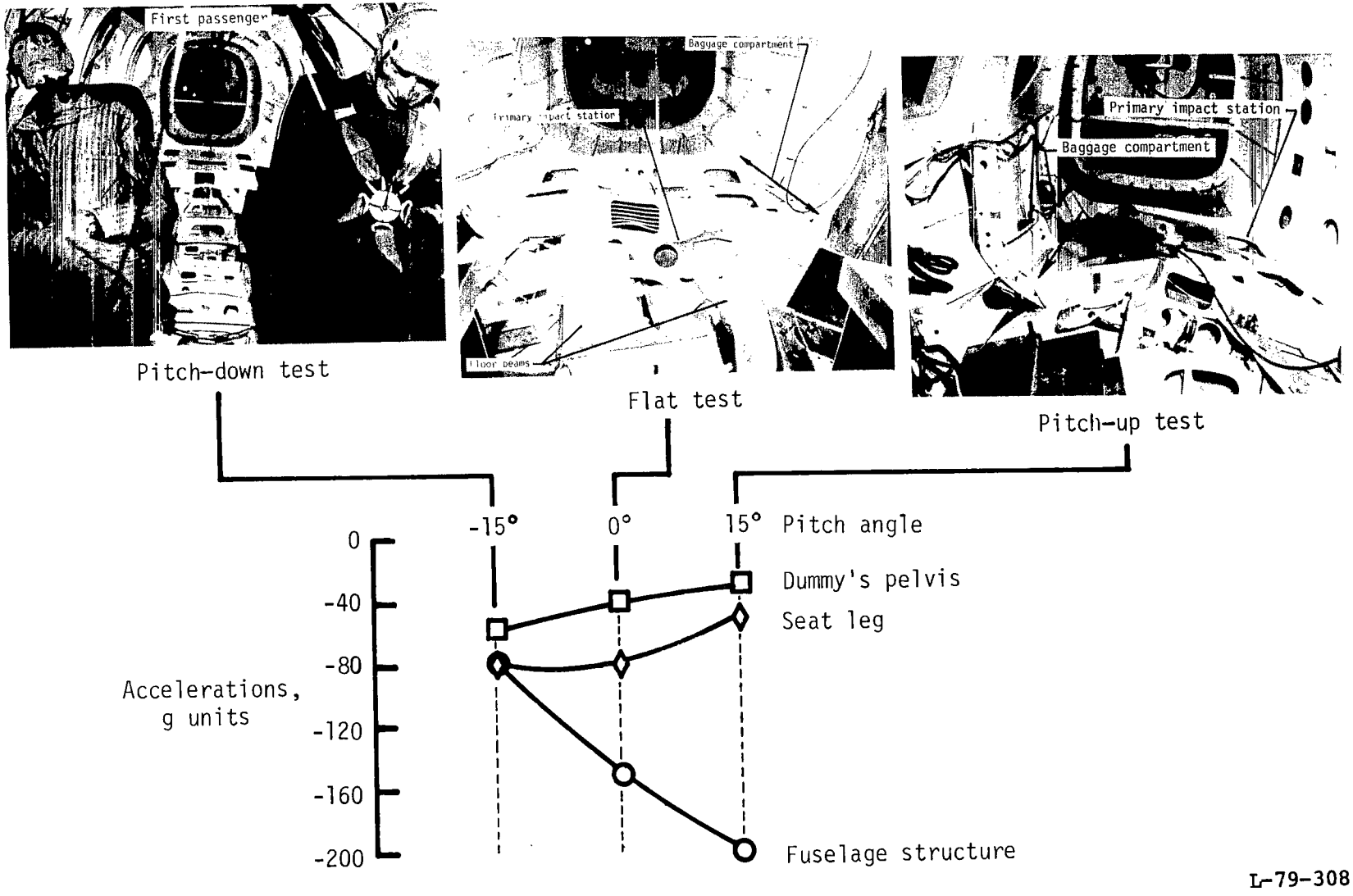

Figure 25.- Maximum normal accelerations in dummy's pelvis, on the floor at the first-passenger seat legs, and on fuselage structure.

1. Report No.	2. Government Accession No.	3. Recipient's Catalog No.
NASA TP-1481		

4. Title and Subtitle	5. Report Date
LIGHT AIRPLANE CRASH TESTS AT THREE PITCH ANGLES	November 1979
	6. Performing Organization Code
7. Author(s)	8. Performing Organization Report No.
Victor L. Vaughan, Jr., and Emilio Alfaro-Bou	L-13051
	10. Work Unit No.
9. Performing Organization Name and Address	505-41-33-01
NASA Langley Research Center Hampton, VA 23665	11. Contract or Grant No.
	13. Type of Report and Period Covered
12. Sponsoring Agency Name and Address	Technical Paper
National Aeronautics and Space Administration Washington, DC 20546	14. Sponsoring Agency Code

15. Supplementary Notes

Technical Film Supplement L-1262 available on request.

16. Abstract

Three similar twin-engine general-aviation airplane specimens were crash tested at the Langley impact dynamics research facility at 27 m/sec, a flight-path angle of -15°, and pitch angles of -15°, 0°, and 15°. Other crash parameters were held constant. The test facility, instrumentation, test specimens, and test method are briefly described. Structural damage and accelerometer data for each of the three impact conditions are presented and discussed.

17. Key Words (Suggested by Author(s))	18. Distribution Statement
Crash worthiness Airplane crash tests Crash damage	Unclassified - Unlimited Subject Category 39

19. Security Classif. (of this report)	20. Security Classif. (of this page)	21. No. of Pages	22. Price*
Unclassified	Unclassified	60	$5.25

* For sale by the National Technical Information Service, Springfield, Virginia 22161

NASA-Langley, 1979

A motion-picture film supplement L-1262 is available on loan. Requests will be filled in the order received. You will be notified of the approximate date scheduled.

The film (16 mm, 10-1/2 min, color, silent) shows various views of three general-aviation airplane specimens at 24 and 400 pps for three pitch angles during the impact sequence.

Requests for the film should be addressed to:

NASA Langley Research Center
Att: Photographic Branch, Mail Stop 425
Hampton, VA 23665

CUT

Date_____

Please send, on loan, copy of film supplement L-1262 to NASA TP-1481.

_____
Name of organization

_____
Street number

_____
City and State Zip code

Attention: Mr._____

Title_____

13 1 10,D, 111979 S00903DS
DEPT OF THE AIR FORCE
AF WEAPONS LABORATORY
ATTN: TECHNICAL LIBRARY (SUL)
KIRTLAND AFB NM 87117